



ARTICLE

Quadratic Finite Volume Element Schemes over Triangular Meshes for a Nonlinear Time-Fractional Rayleigh-Stokes Problem

Yanlong Zhang¹, Yanhui Zhou² and Jiming Wu^{3,*}

¹Graduate School of China Academy of Engineering Physics, Beijing, 100088, China

²School of Data and Computer Science, Sun Yat-Sen University, Guangzhou, 510275, China

³Institute of Applied Physics and Computational Mathematics, Beijing, 100088, China

*Corresponding Author: Jiming Wu. Email: wu_jiming@iapcm.ac.cn

Received: 11 November 2020 Accepted: 15 January 2021

ABSTRACT

In this article, we study a 2D nonlinear time-fractional Rayleigh-Stokes problem, which has an anomalous sub-diffusion term, on triangular meshes by quadratic finite volume element schemes. Time-fractional derivative, defined by Caputo fractional derivative, is discretized through $L2 - 1_\sigma$ formula, and a two step scheme is used to approximate the time first-order derivative at time $t_{n-\alpha/2}$, where the nonlinear term is approximated by using a matching linearized difference scheme. A family of quadratic finite volume element schemes with two parameters are proposed for the spatial discretization, where the range of values for two parameters are $\beta_1 \in (0, 1/2)$, $\beta_2 \in (0, 2/3)$. For testing the precision of numerical algorithms, we calculate some numerical examples which have known exact solution or unknown exact solution by several kinds of quadratic finite volume element schemes, and contrast with the results of an existing quadratic finite element scheme by drawing diversified comparison plots and showing the detailed data of L^2 error results and convergence orders. Numerical results indicate that, L^2 error estimate of one scheme with parameters $\beta_1 = (3 - \sqrt{3})/6$, $\beta_2 = (6 + \sqrt{3} - \sqrt{21 + 6\sqrt{3}})/9$ is $\mathcal{O}(h^3 + \Delta t^2)$, and L^2 error estimates of other schemes are $\mathcal{O}(h^2 + \Delta t^2)$, where h and Δt denote the spatial and temporal discretization parameters, respectively.

KEYWORDS

Quadratic finite volume element schemes; anomalous sub-diffusion term; L^2 error estimate; quadratic finite element scheme

1 Introduction

Recently, due to the widespread use of fractional partial differential equations (FPDEs), such as dispersion in a porous medium, statistical mechanics, mathematical biology and so on, numerical solution of FPDEs becomes one of the frontier fields in the research. Fractional partial differential equations can be roughly classified into three categories: Space FPDEs [1–10], time FPDEs [11–29] and space-time FPDEs [30–34]. Anomalous sub-diffusion equations, one type of time FPDEs, arise in some physical and biological processes. And the study of FPDEs



This work is licensed under a Creative Commons Attribution 4.0 International License, which permits unrestricted use, distribution, and reproduction in any medium, provided the original work is properly cited.

with anomalous sub-diffusion terms, such as modified anomalous sub-diffusion equations [17,18], fractional Cable equations [11,16] or others, is also meaningful and popular. The problem considered in this article, which belongs to a nonlinear time-fractional Rayleigh-Stokes problem [19–22] applied in some non-Newtonian fluids, is a variant of the Stokes' first problems and Rayleigh-Stokes problems [35–38], and it is important in physics and engineering.

At present, numerical simulation is an important and effective way to solve partial differential equations, and the relevant numerical methods can be finite difference methods [7,8,14–17], finite element methods (FEMs) [1,2,9,11–13,21,29,31–33,39], meshless methods [40,41], finite volume methods [3–6,42–54] and so on. Of course, the research for FPDEs by finite volume element methods (FVEMs) [10,23–28] has no exception for the local conservation and simple implementation. Sayevand et al. [23] presented a spatially semi-discrete piecewise linear FVEM for the time-fractional sub-diffusion problem and obtained some error estimates of the solution in both FEMs and FVEMs. A linear finite volume element scheme for the 2D time-fractional anomalous sub-diffusion equations was studied and analyzed by Karaa et al. [24], where the convergence rate was of order $h^2 + \Delta t^{1+\alpha}$ in the $L^\infty(L^2)$ norm and the results were improved in [25] for both smooth and nonsmooth initial data. Badr et al. [26] proposed a linear FVEM for the time-fractional advection diffusion problem in one-dimension, and proved that the fully discrete scheme is unconditionally stable. Furthermore, Yazdani et al. [10] solved a space-fractional advection-dispersion problem in one-dimension by using linear FVEM and proved it is stable when the mesh grid size is small enough. Zhao et al. [27] constructed a mixed finite volume element scheme for the time-fractional reaction-diffusion equation, and showed the unconditional stability analysis for it. Moreover, Zhao et al. [28] proposed a linear FVEM for the nonlinear time-fractional mobile/immobile transport equations on triangular grids, and obtained the optimal priori error estimates in $L^\infty(L^2)$ and $L^2(H^1)$ norms. To our knowledge, the study of high order finite volume element methods for 2D FPDEs is undiscovered.

There are some research about quadratic finite volume element methods for solving partial differential equations on triangular meshes. Tian et al. [42] presented quadratic element generalized differential methods to solve elliptic equations where two parameters of the quadratic element were $\beta_1 = \beta_2 = 1/3$ (referring to the definition Eqs. (4), (5)). Liebau [43] solved one type of elliptic boundary value problems by a quadratic element scheme with parameters $\beta_1 = 1/4$, $\beta_2 = 1/3$, and proved $\mathcal{O}(h^2)$ error estimate under some assumption conditions. Xu et al. [44] started to study the structure about two parameters of the quadratic element, and improved some existing coercivity results. Chen et al. [45] established a general framework for construction and analysis of the higher-order finite volume methods. Wang et al. [46] established a unified framework to perform the L^2 error analysis for high order finite volume methods on triangular meshes, and proposed a new quadratic scheme with parameters $\beta_1 = (3 - \sqrt{3})/6$, $\beta_2 = (6 + \sqrt{3} - \sqrt{21 + 6\sqrt{3}})/9$ to achieve the optimal L^2 convergence order. An unconditionally stable quadratic finite volume scheme with parameters $\beta_1 = \beta_2 = (3 - \sqrt{3})/6$ for elliptic equations was presented by Zou [47], and it had optimal convergence orders under H^1 norms. For the quadratic finite volume element schemes with parameters $\beta_1 = (3 - \sqrt{3})/6$, $\beta_2 \in (0, 2/3)$, Zhou et al. [48] obtained an analytic minimum angle condition and an optimal H^1 error estimates under the improved coercivity result. Moreover, a unified framework for the coercivity analysis of a class of quadratic schemes with parameters $\beta_1 \in (0, 1/2)$, $\beta_2 \in (0, 2/3)$ was established for elliptic boundary value problems [49], which covered all the existing quadratic schemes of Lagrange type, and minimum angle conditions of the existing literatures are improved. All the above papers are mainly confined to the elliptic problems and we have seen some applications to other problems [50–53], but none relevant study for FPDEs.

In this article, the quadratic finite volume element method is proposed to solve one class of FPDEs, that is, a 2D nonlinear time-fractional Rayleigh-Stokes problem with the time-fractional derivative defined by Caputo fractional derivative. In spatial direction, this problem is solved by a class of quadratic finite volume element schemes with two parameters β_1 and β_2 . Moreover, this problem is discretized at time $t_{n-\alpha/2}$ and the time-fractional derivative is discretized through $L2 - 1_\sigma$ formula in time direction. Numerical experiments indicate the efficiency of the schemes, specifically, the L^2 error estimate of one scheme is $\mathcal{O}(h^3 + \Delta t^2)$, and L^2 error estimates of other schemes are $\mathcal{O}(h^2 + \Delta t^2)$. We find that the new finite volume element schemes are comparable with an existing finite element scheme [29].

The outline of this paper is as follows. In Section 2, we describe in details the specific algorithm steps of the quadratic finite volume element schemes over triangular meshes, and finally obtain the fully discrete schemes. In Section 3, some numerical experiments are performed to investigate the performance of the quadratic finite volume element schemes. The numerical results are also compared with those of an existing quadratic finite element scheme. A brief conclusion ends this article in last section.

2 Quadratic Finite Volume Element Schemes

2.1 Preliminary

In this article, we construct a family of quadratic finite volume element schemes to solve the following 2D nonlinear time-fractional Rayleigh-Stokes problem:

$$\frac{\partial u(\mathbf{x}, t)}{\partial t} - \frac{\partial^\alpha \Delta u(\mathbf{x}, t)}{\partial t^\alpha} - \Delta u(\mathbf{x}, t) = f(u) + g(\mathbf{x}, t), \quad (\mathbf{x}, t) \in \Omega \times (0, T], \quad (1)$$

$$u(\mathbf{x}, t) = 0, \quad (\mathbf{x}, t) \in \partial\Omega \times (0, T], \quad (2)$$

$$u(\mathbf{x}, 0) = u_0(\mathbf{x}), \quad \mathbf{x} \in \Omega, \quad (3)$$

where $\mathbf{x} = (x, y) \in \Omega \subset \mathbb{R}^2$ and

$$\frac{\partial^\alpha \Delta u(\mathbf{x}, t)}{\partial t^\alpha} = \frac{1}{\Gamma(1-\alpha)} \int_0^t \frac{\partial \Delta u(\mathbf{x}, \tau)}{\partial \tau} \frac{d\tau}{(t-\tau)^\alpha},$$

denotes the Caputo fractional derivative of order $\alpha \in (0, 1)$, which is an anomalous sub-diffusion term. $f(u)$ is a nonlinear term subjected to the following conditions, $|f(u)| \leq C_1|u|$ and $|f'(u)| \leq C_2$ where C_1 and C_2 are positive constants, and $g(\mathbf{x}, t)$ is the source term.

For the numerical solution of Eqs. (1)–(3), the space domain Ω is first triangulated to get the so-called primary mesh \mathcal{T}_h , see the solid line segments in Fig. 1. The trial function space U_h is then defined with respect to \mathcal{T}_h , given by

$$U_h = \{u_h \in C(\bar{\Omega}): u_h|_K \in \mathbb{P}_2, \forall K \in \mathcal{T}_h, u_h|_{\partial\Omega} = 0\},$$

where K denotes a generic triangular element and \mathbb{P}_2 is the set of all polynomials of degree less than or equal to 2. It is easy to see that U_h is the same one as that of the standard quadratic finite element method, but the test function space here is different.

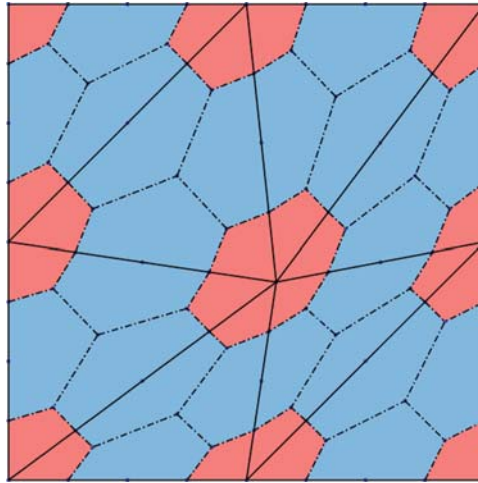


Figure 1: The primary mesh and dual mesh

In order to define the test function space, we need to construct a dual mesh associated with \mathcal{T}_h , see the dashed line segments in Fig. 1. For any triangular element $K = \Delta P_1 P_2 P_3$ with $P_1 = (x_1, y_1)$, $P_2 = (x_2, y_2)$ and $P_3 = (x_3, y_3)$, we denote the barycenter of K as Q , and the midpoints of the three sides as M_1 , M_2 and M_3 , respectively, see Fig. 2. $G_{k,k+1}$ and $G_{k+1,k}$ are the two points on $P_k P_{k+1}$, satisfying

$$\frac{|P_k G_{k,k+1}|}{|P_k P_{k+1}|} = \frac{|G_{k+1,k} P_{k+1}|}{|P_k P_{k+1}|} = \beta_1 \in \left(0, \frac{1}{2}\right), \quad (4)$$

while $P_{k,k+1}$ is a point on $P_k M_{k+1}$ such that

$$\frac{|P_k P_{k,k+1}|}{|P_k M_{k+1}|} = \beta_2 \in \left(0, \frac{2}{3}\right), \quad (5)$$

where k is a periodic index with Period 3. Using the above notations, K can be further partitioned into six subcells, i.e., three quadrilaterals and three pentagons, see Fig. 2. Let \mathcal{N}_h be the set of all vertices and edge midpoints on the primary mesh \mathcal{T}_h . Then, K_P^* , the dual cell associated with $P \in \mathcal{N}_h$, is defined as the union of the subcells sharing P , and the dual mesh is defined as $\mathcal{T}_h^* = \{K_P^* : \forall P \in \mathcal{N}_h\}$. Now, the test function space is chosen as

$$V_h = \{v_h \in L^2(\bar{\Omega}) : v_h|_{K_P^*} = \text{constant}, \forall P \in \mathcal{N}_h^\circ; v_h|_{K_P^*} = 0, \forall P \in \mathcal{N}_h \cap \partial\Omega\},$$

where $\mathcal{N}_h^\circ = \mathcal{N}_h \setminus \partial\Omega$. Here we remark that the dual mesh \mathcal{T}_h^* and the test function space V_h depend on two parameters β_1 and β_2 . Different choices of the pair (β_1, β_2) lead to different finite volume element schemes.

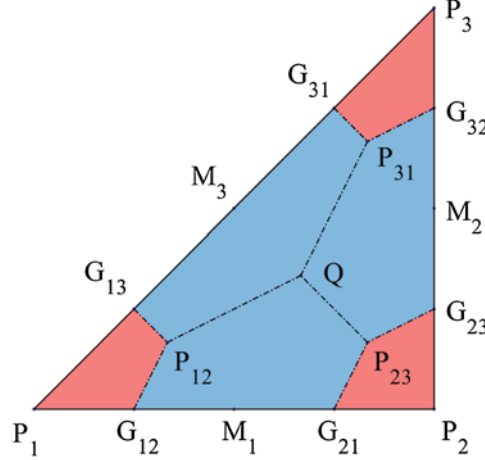


Figure 2: Partition of the triangular element K

2.2 Semi-Discrete Schemes

In this part, we propose the following spatial discrete formulation of Eq. (1),

$$\int_{\Omega} \left(\frac{\partial u}{\partial t} - \frac{\partial^\alpha \Delta u}{\partial t^\alpha} - \Delta u \right) v_h dx dy = \int_{\Omega} (f(u) + g) v_h dx dy, \quad \forall v_h \in V_h.$$

By the divergence theorem and the definition of V_h , we have,

$$\int_{K_P^*} \frac{\partial u}{\partial t} dx dy - \int_{\partial K_P^*} \left(\frac{\partial^\alpha \nabla u}{\partial t^\alpha} \cdot \mathbf{n}_P^* + \nabla u \cdot \mathbf{n}_P^* \right) ds = \int_{K_P^*} (f(u) + g) dx dy, \quad \forall P \in \mathcal{N}_h^\circ, \quad (6)$$

where ∇ is the gradient operator and \mathbf{n}_P^* is the unit normal vector outward to ∂K_P^* . The left hand-side of Eq. (6) can be rewritten as

$$\int_{K_P^*} \frac{\partial u}{\partial t} dx dy - \int_{\partial K_P^*} \left(\frac{\partial^\alpha \nabla u}{\partial t^\alpha} \cdot \mathbf{n}_P^* + \nabla u \cdot \mathbf{n}_P^* \right) ds = \sum_{K \in \mathcal{T}_h} \left[\int_{K_P} \frac{\partial u}{\partial t} dx dy - \int_{\varepsilon_{K,P}} \left(\frac{\partial^\alpha \nabla u}{\partial t^\alpha} + \nabla u \right) ds \cdot \mathbf{n}_P^* \right],$$

where $K_P = K \cap K_P^*$ and $\varepsilon_{K,P} = K \cap \partial K_P^*$. Based on the above formulation, we formulate the semi-discrete finite volume element solution of the Eq. (6) as: Find $u_h = u_h(x, y, t) \in U_h$ with $t \in (0, T]$, such that

$$\sum_{K \in \mathcal{T}_h} \left[\int_{K_P} \frac{\partial u_h}{\partial t} dx dy - \int_{\varepsilon_{K,P}} \left(\frac{\partial^\alpha \nabla u_h}{\partial t^\alpha} + \nabla u_h \right) ds \cdot \mathbf{n}_P^* \right] = \sum_{K \in \mathcal{T}_h} \int_{K_P} (f(u_h) + g) dx dy, \quad \forall P \in \mathcal{N}_h^\circ. \quad (7)$$

For the computation of the terms in Eq. (7), we introduce the following affine mapping that transforms K onto \hat{K} in (λ_1, λ_2) plane,

$$\begin{cases} \lambda_1 = \frac{1}{J_K} \left(\begin{vmatrix} y_2 & 1 \\ y_3 & 1 \end{vmatrix} x - \begin{vmatrix} x_2 & 1 \\ x_3 & 1 \end{vmatrix} y + \begin{vmatrix} x_2 & y_2 \\ x_3 & y_3 \end{vmatrix} \right), \\ \lambda_2 = \frac{1}{J_K} \left(\begin{vmatrix} y_3 & 1 \\ y_1 & 1 \end{vmatrix} x - \begin{vmatrix} x_3 & 1 \\ x_1 & 1 \end{vmatrix} y + \begin{vmatrix} x_3 & y_3 \\ x_1 & y_1 \end{vmatrix} \right), \end{cases} \quad (8)$$

where

$$J_K = \begin{vmatrix} x_1 & y_1 & 1 \\ x_2 & y_2 & 1 \\ x_3 & y_3 & 1 \end{vmatrix},$$

and \hat{K} is the reference element whose vertices and barycenter are specified by $\hat{P}_1 = (1, 0)$, $\hat{P}_2 = (0, 1)$, $\hat{P}_3 = (0, 0)$ and $\hat{Q} = (1/3, 1/3)$, respectively, see Fig. 3. Let $u_{h,K}$ be the restriction of u_h on K . Then, under the affine mapping Eq. (8), the counterparts of u_h and $u_{h,K}$ can be expressed as

$$\hat{u}_h = \hat{u}_h(\lambda_1, \lambda_2, t), \quad \hat{u}_{h,\hat{K}} = \sum_{j=1}^6 u_{j,K} \hat{\phi}_j(\lambda_1, \lambda_2),$$

where

$$u_{j,K} = u_h(P_j), \quad u_{j+3,K} = u_h(M_j), \quad j = 1, 2, 3,$$

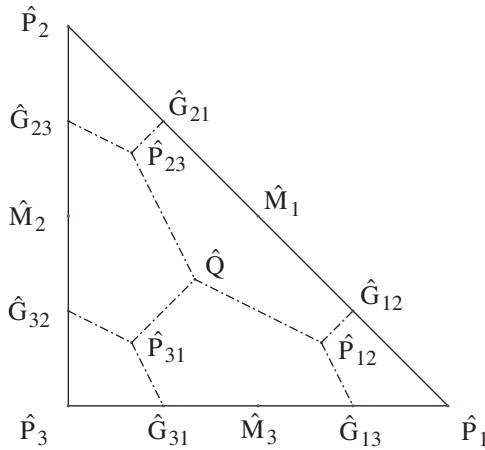


Figure 3: The reference element \hat{K} and its associated subcells

$\hat{\phi}_j(\lambda_1, \lambda_2) (1 \leq j \leq 6)$ are the shape functions on \hat{K} , given by

$$\begin{cases} \hat{\phi}_1(\lambda_1, \lambda_2) = \lambda_1(2\lambda_1 - 1), & \hat{\phi}_2(\lambda_1, \lambda_2) = \lambda_2(2\lambda_2 - 1), \\ \hat{\phi}_3(\lambda_1, \lambda_2) = \lambda_3(2\lambda_3 - 1), & \hat{\phi}_4(\lambda_1, \lambda_2) = 4\lambda_1\lambda_2, \\ \hat{\phi}_5(\lambda_1, \lambda_2) = 4\lambda_2\lambda_3, & \hat{\phi}_6(\lambda_1, \lambda_2) = 4\lambda_1\lambda_3, \end{cases}$$

and $\lambda_3 = 1 - \lambda_1 - \lambda_2$. Now we rewrite Eq. (7) to get the following semi-discrete schemes,

$$\sum_{K \in \mathcal{T}_h} \left[\int_{\hat{K}_P} \frac{\partial \hat{u}_h}{\partial t} J_K d\lambda_1 d\lambda_2 - \int_{\hat{\epsilon}_{K,P}} \left(\frac{\partial^\alpha \nabla \hat{u}_h}{\partial t^\alpha} + \nabla \hat{u}_h \right) F_{K,P} dl \cdot \mathbf{n}_P^* \right] = \sum_{K \in \mathcal{T}_h} \int_{\hat{K}_P} (f(\hat{u}_h) + \hat{g}) J_K d\lambda_1 d\lambda_2, \quad (9)$$

where $P \in \mathcal{N}_h^\circ$ and $F_{K,P}$ denotes the ratio of the measures of $\varepsilon_{K,P}$ and $\hat{\varepsilon}_{K,P}$. One can see that $\nabla \hat{u}_{h,\hat{K}} = \sum_{j=1}^6 u_{j,K} \nabla \hat{\phi}_j$, where

$$\nabla \hat{\phi}_j = \begin{pmatrix} \frac{\partial \hat{\phi}_j}{\partial x} \\ \frac{\partial \hat{\phi}_j}{\partial y} \end{pmatrix} = \begin{pmatrix} \frac{\partial \hat{\phi}_j}{\partial \lambda_1} \frac{\partial \lambda_1}{\partial x} + \frac{\partial \hat{\phi}_j}{\partial \lambda_2} \frac{\partial \lambda_2}{\partial x} \\ \frac{\partial \hat{\phi}_j}{\partial \lambda_1} \frac{\partial \lambda_1}{\partial y} + \frac{\partial \hat{\phi}_j}{\partial \lambda_2} \frac{\partial \lambda_2}{\partial y} \end{pmatrix} = \begin{pmatrix} \frac{\partial \lambda_1}{\partial x} & \frac{\partial \lambda_2}{\partial x} \\ \frac{\partial \lambda_1}{\partial y} & \frac{\partial \lambda_2}{\partial y} \end{pmatrix} \widehat{\nabla} \hat{\phi}_j,$$

and $\widehat{\nabla}$ is the gradient operator with respect to (λ_1, λ_2) plane. By straightforward calculations, we have

$$\begin{aligned} \widehat{\nabla} \hat{\phi}_1 &= \begin{pmatrix} 4\lambda_1 - 1 \\ 0 \end{pmatrix}, & \widehat{\nabla} \hat{\phi}_2 &= \begin{pmatrix} 0 \\ 4\lambda_2 - 1 \end{pmatrix}, & \widehat{\nabla} \hat{\phi}_3 &= \begin{pmatrix} 4\lambda_1 + 4\lambda_2 - 3 \\ 4\lambda_1 + 4\lambda_2 - 3 \end{pmatrix}, \\ \widehat{\nabla} \hat{\phi}_4 &= 4 \begin{pmatrix} \lambda_2 \\ \lambda_1 \end{pmatrix}, & \widehat{\nabla} \hat{\phi}_5 &= 4 \begin{pmatrix} -\lambda_2 \\ -\lambda_1 - 2\lambda_2 + 1 \end{pmatrix}, & \widehat{\nabla} \hat{\phi}_6 &= 4 \begin{pmatrix} -2\lambda_1 - \lambda_2 + 1 \\ -\lambda_1 \end{pmatrix}. \end{aligned}$$

2.3 Fully Discrete Schemes

Next we introduce the fully discrete schemes at time $t_{n-\alpha/2}$. Let $0 = t_0 < t_1 < \dots < t_N = T$ be a uniform partition of the time interval $[0, T]$ with mesh length $\Delta t = T/N$, and $t_n = n\Delta t$ ($n = 0, 1, 2, \dots, N$). For any function $z(t)$, let $z^n = z(t_n)$.

Lemma 2.1. ([14], Lemma 2) Suppose $z(t) \in C^3[0, T]$. Then, we have

$$\frac{\partial z}{\partial t}(t_{n-\frac{\alpha}{2}}) = \begin{cases} \frac{1}{\Delta t}(z^1 - z^0) + \mathcal{O}(\Delta t), & n=1, \\ \frac{1}{2\Delta t} \left[(3-\alpha)z^n - (4-2\alpha)z^{n-1} + (1-\alpha)z^{n-2} \right] + \mathcal{O}(\Delta t^2), & n \geq 2. \end{cases} \quad (10)$$

Lemma 2.2. ([11], Lemma 2) Assume that $f(t) \in C^2[0, T]$. Then, the following second-order formula for the approximation of the nonlinear term at time $t_{n-\alpha/2}$ holds,

$$f(z(t_{n-\frac{\alpha}{2}})) = \left(2 - \frac{\alpha}{2}\right) f(z^{n-1}) - \left(1 - \frac{\alpha}{2}\right) f(z^{n-2}) + \mathcal{O}(\Delta t^2), \quad n \geq 2. \quad (11)$$

Lemma 2.3. ([15], Lemma 2) Suppose $z(t) \in C^3[0, T]$. We have the following $L2 - 1_\sigma$ formula at time $t_{n-\alpha/2}$,

$$\frac{\partial^\alpha z}{\partial t^\alpha}(t_{n-\frac{\alpha}{2}}) = \frac{\Delta t^{-\alpha}}{\Gamma(2-\alpha)} \left[c_0^n z^n - \sum_{j=1}^{n-1} (c_{n-j-1}^n - c_{n-j}^n) z^j - c_{n-1}^n z^0 \right] + \mathcal{O}(\Delta t^{3-\alpha}), \quad (12)$$

where $c_0^1 = a_0$, for $n=1$, and for $n \geq 2$,

$$c_l^n = \begin{cases} a_0 + b_1, & l=0, \\ a_l + b_{l+1} - b_l, & 1 \leq l \leq n-2, \\ a_l - b_l, & l=n-1, \end{cases}$$

with

$$\begin{aligned} a_0 &= \left(1 - \frac{\alpha}{2}\right)^{1-\alpha}, \quad a_l = \left(l + 1 - \frac{\alpha}{2}\right)^{1-\alpha} - \left(l - \frac{\alpha}{2}\right)^{1-\alpha}, \quad l \geq 1, \\ b_l &= \frac{1}{2-\alpha} \left[\left(l + 1 - \frac{\alpha}{2}\right)^{2-\alpha} - \left(l - \frac{\alpha}{2}\right)^{2-\alpha} \right] - \frac{1}{2} \left[\left(l + 1 - \frac{\alpha}{2}\right)^{1-\alpha} + \left(l - \frac{\alpha}{2}\right)^{1-\alpha} \right], \quad l \geq 1. \end{aligned}$$

Based on Lemmas 2.1–2.3, we propose the following fully discrete schemes by the Eq. (9) at time $t_{n-\alpha/2}$:

for $n = 1$,

$$\begin{aligned} &\sum_{K \in \mathcal{T}_h} \left\{ \int_{\hat{K}_P} \frac{1}{\Delta t} (\hat{u}_h^1 - \hat{u}_h^0) J_K d\lambda_1 d\lambda_2 - \int_{\hat{\varepsilon}_{K,P}} \left[\frac{c_0^1 \Delta t^{-\alpha}}{\Gamma(2-\alpha)} (\nabla \hat{u}_h^1 - \nabla \hat{u}_h^0) + \left(\left(1 - \frac{\alpha}{2}\right) \nabla \hat{u}_h^1 + \frac{\alpha}{2} \nabla \hat{u}_h^0 \right) \right] \mathbf{F}_{K,P} dl \cdot \mathbf{n}_P^* \right\} \\ &= \sum_{K \in \mathcal{T}_h} \int_{\hat{K}_P} \left(f(\hat{u}_h^0) + \hat{g}^{1-\frac{\alpha}{2}} \right) J_K d\lambda_1 d\lambda_2, \quad \forall P \in \mathcal{N}_h^\circ; \end{aligned} \quad (13)$$

for $n \geq 2$,

$$\begin{aligned} &\sum_{K \in \mathcal{T}_h} \left\{ \int_{\hat{K}_P} \frac{1}{2\Delta t} \left((3-\alpha) \hat{u}_h^n - (4-2\alpha) \hat{u}_h^{n-1} + (1-\alpha) \hat{u}_h^{n-2} \right) J_K d\lambda_1 d\lambda_2 \right. \\ &\quad \left. - \int_{\hat{\varepsilon}_{K,P}} \left[\frac{\Delta t^{-\alpha}}{\Gamma(2-\alpha)} \left(c_0^n \nabla \hat{u}_h^n - \sum_{j=1}^{n-1} (c_{n-j-1}^n - c_{n-j}^n) \nabla \hat{u}_h^j - c_{n-1}^n \nabla \hat{u}_h^0 \right) + \left(\left(1 - \frac{\alpha}{2}\right) \nabla \hat{u}_h^n + \frac{\alpha}{2} \nabla \hat{u}_h^{n-1} \right) \right] \right. \\ &\quad \times \mathbf{F}_{K,P} dl \cdot \mathbf{n}_P^* \left. \right\} = \sum_{K \in \mathcal{T}_h} \int_{\hat{K}_P} \left[\left(\left(2 - \frac{\alpha}{2}\right) f(\hat{u}_h^{n-1}) - \left(1 - \frac{\alpha}{2}\right) f(\hat{u}_h^{n-2}) \right) + \hat{g}^{n-\frac{\alpha}{2}} \right] J_K d\lambda_1 d\lambda_2, \quad \forall P \in \mathcal{N}_h^\circ, \end{aligned} \quad (14)$$

where $\hat{u}_h^n = \hat{u}_h^n(\lambda_1, \lambda_2, t_n)$, $n = 0, 1, \dots, N$.

Let the basis functions of the trial function space U_h be denoted as $\varphi_k(x, y)$, ($k = 1, 2, \dots, m$) where m is the number of unknowns (i.e., $m = \#\mathcal{N}_h^\circ$), then the numerical solution $u_h^n = (\varphi_1, \varphi_2, \dots, \varphi_m) \cdot \mathbf{u}_h^n \in U_h$, where the vector $\mathbf{u}_h^n = (u_1^n, u_2^n, \dots, u_m^n)^T$, ($n = 0, 1, \dots, N$). Moreover, we know $\hat{u}_h^n = (\hat{\varphi}_1, \hat{\varphi}_2, \dots, \hat{\varphi}_m) \cdot \mathbf{u}_h^n$, where $\hat{\varphi}_k(\lambda_1, \lambda_2)$, ($k = 1, 2, \dots, m$) are transformed from $\varphi_k(x, y)$, ($k = 1, 2, \dots, m$) by the affine mapping Eq. (8). By simplifying and synthesizing the Eqs. (13), (14), we obtain the following matrix form of the fully discrete schemes:

for $n = 1$,

$$\mathbf{M}\mathbf{u}_h^1 - \left[\frac{c_0^1 \Delta t^{1-\alpha}}{\Gamma(2-\alpha)} + \Delta t \left(1 - \frac{\alpha}{2}\right) \right] \mathbf{A}\mathbf{u}_h^1 = \Delta t \mathbf{M}\mathbf{f}^0 + \Delta t \mathbf{g}^{1-\frac{\alpha}{2}} + \mathbf{M}\mathbf{u}_h^0 - \frac{c_0^1 \Delta t^{1-\alpha}}{\Gamma(2-\alpha)} \mathbf{A}\mathbf{u}_h^0 + \Delta t \frac{\alpha}{2} \mathbf{A}\mathbf{u}_h^0; \quad (15)$$

for $n \geq 2$,

$$(3 - \alpha)\mathbf{M}\mathbf{u}_h^n - \left[\frac{2c_0^n \Delta t^{1-\alpha}}{\Gamma(2-\alpha)} + 2\Delta t \left(1 - \frac{\alpha}{2}\right) \right] \mathbf{A}\mathbf{u}_h^n = 2\Delta t \mathbf{M} \left[\left(2 - \frac{\alpha}{2}\right) \mathbf{f}^{n-1} - \left(1 - \frac{\alpha}{2}\right) \mathbf{f}^{n-2} \right] + 2\Delta t \mathbf{g}^{n-\frac{\alpha}{2}} \\ + (4 - 2\alpha)\mathbf{M}\mathbf{u}_h^{n-1} - (1 - \alpha)\mathbf{M}\mathbf{u}_h^{n-2} - \frac{2\Delta t^{1-\alpha}}{\Gamma(2-\alpha)} \mathbf{A} \left[\sum_{j=1}^{n-1} (c_{n-j-1}^n - c_{n-j}^n) \mathbf{u}_h^j + c_{n-1}^n \mathbf{u}_h^0 \right] + \Delta t \alpha \mathbf{A}\mathbf{u}_h^{n-1}, \quad (16)$$

where

$$\mathbf{f}^n = (f_k^n)_{m \times 1}, \quad f_k^n = f(u_h^n(P_k)), \quad P_k \in \mathcal{N}_h^\circ, \quad (17)$$

$$\mathbf{g}^{n-\frac{\alpha}{2}} = \left(g_k^{n-\frac{\alpha}{2}} \right)_{m \times 1}, \quad g_k^{n-\frac{\alpha}{2}} = \sum_{K \in \mathcal{T}_h} \int_{\hat{K}_{P_k}} \hat{g}^{n-\frac{\alpha}{2}} J_K d\lambda_1 d\lambda_2, \quad P_k \in \mathcal{N}_h^\circ, \quad (18)$$

mass matrix $\mathbf{M} = \sum_{K \in \mathcal{T}_h} \mathbf{M}_K$ and stiffness matrix $\mathbf{A} = \sum_{K \in \mathcal{T}_h} \mathbf{A}_K$. Meanwhile, \mathbf{M}_K and \mathbf{A}_K , square matrices of degree m , are expanded by the element matrices \mathbb{M}_K and \mathbb{A}_K as follows:

$$\mathbb{M}_K = (m_{ij})_{6 \times 6}, \quad m_{ij} = \int_{\hat{K}_{P_i}} \hat{\phi}_j J_K d\lambda_1 d\lambda_2, \quad (19)$$

$$\mathbb{A}_K = (a_{ij})_{6 \times 6}, \quad a_{ij} = \int_{\hat{K}_{P_i}} \nabla \hat{\phi}_j \mathbf{F}_{K,P} dl \cdot \mathbf{n}_{P_i}^*, \quad (20)$$

where $K_{P_i} = K \cap K_{P_i}^*$ and $\varepsilon_{K,P_i} = K \cap \partial K_{P_i}^*$ are transformed to \hat{K}_{P_i} and $\hat{\varepsilon}_{K,P_i}$ by the affine mapping Eq. (8) and P_i ($i = 1, \dots, 6$) ($P_{j+3} = M_j$, $j = 1, 2, 3$) are vertices or edge midpoints of the element K .

For the above finite volume element schemes, we emphasize that the nonlinear term is approximated by using the linearized difference scheme in Lemma 2.2, and none nonlinear iteration is involved. The whole algorithm is summarized below.

Algorithm 1: The quadratic finite volume element schemes (15)–(20)

Step 1: Set $n = 0$ and compute $\mathbf{u}_h^0 = u_0(\mathbf{x})$ by using the initial condition in (3);

Step 2: Set $n = 1$ and compute \mathbf{f}^0 by the expression $f(u)$ and (17). Then, solve the linear system (15) to obtain \mathbf{u}_h^1 ;

Step 3: Do $n = 2$ to N

 Compute \mathbf{f}^{n-1} and \mathbf{f}^{n-2} by using the expression $f(u)$ and (17);

 Obtain \mathbf{u}_h^n by solving the linear system (16);

End do

3 Numerical Examples

In this section, we use Eqs. (15)–(20) to solve four examples on uniform triangular mesh (Mesh I) and random triangular mesh (Mesh II), respectively, see Figs. 4, 5. The first level of

Mesh II is constructed from Mesh I by the following random distortion of the interior vertices,
 $x := x + \omega \eta_x h, \quad y := y + \omega \eta_y h,$

where $\omega \in (0, 0.5)$ is the disturbance coefficient, h is the spatial mesh size, η_x and η_y are two random numbers located in $[-1, 1]$. The subsequent level is refined by the standard bisection procedure from its previous level. In our numerical examples, we choose the disturbance coefficient $\omega = 0.2$ for Mesh II (see Fig. 5). Recall that our quadratic finite volume element schemes have two parameters β_1 and β_2 . Here we just investigate the following specific schemes:

- First scheme (QFVE-1): $\beta_1 = (3 - \sqrt{3})/6, \beta_2 = (6 + \sqrt{3} - \sqrt{21 + 6\sqrt{3}})/9;$
- Second scheme (QFVE-2): $\beta_1 = \beta_2 = (3 - \sqrt{3})/6;$
- Third scheme (QFVE-3): $\beta_1 = 1/4, \beta_2 = 1/3;$
- Fourth scheme (QFVE-4): $\beta_1 = \beta_2 = 1/3.$

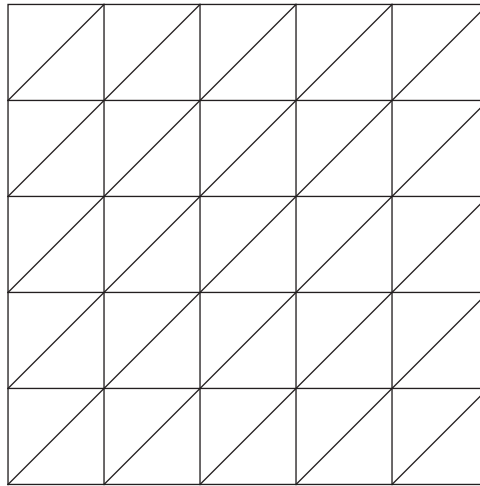


Figure 4: Uniform triangular mesh (Mesh I)

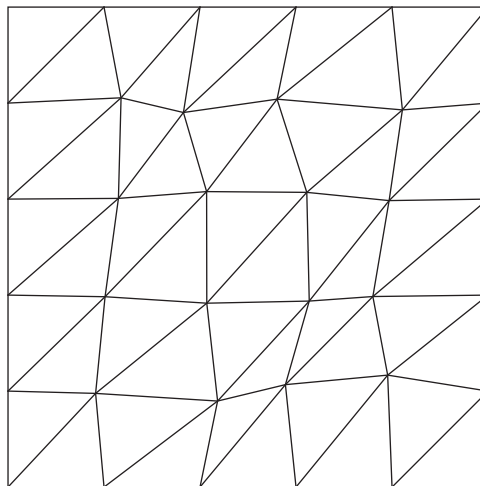


Figure 5: Random triangular mesh (Mesh II)

We remark that the counterparts of the above schemes for elliptic problems have been studied in [42,43,46,47], respectively. The L^2 errors E_u and convergence orders R_u^1, R_u^2 are defined as

$$E_u = \max_{1 \leq n \leq N} \left(\sum_{K \in \mathcal{T}_h} \int_K (u_h(x, y, t_n) - u(x, y, t_n))^2 dx dy \right)^{\frac{1}{2}},$$

$$R_u^1 = \frac{\log(E_u(h_2)/E_u(h_1))}{\log(h_2/h_1)}, \quad R_u^2 = \frac{\log(E_u(\Delta t_2)/E_u(\Delta t_1))}{\log(\Delta t_2/\Delta t_1)},$$

respectively, where h_1 and h_2 are the spatial mesh sizes of two successive meshes, and Δt_1 and Δt_2 are the mesh sizes of two successive time levels. Moreover, the results of the quadratic finite element scheme (QFE) [29] are also employed for comparison.

3.1 Example 1

Solve Eqs. (1)–(3) with the nonlinear term $f(u) = u^2$ and the source term

$$g(\mathbf{x}, t) = \left[(3 + \alpha)t^{2+\alpha} + 8\pi^2 t^{3+\alpha} + \frac{4\pi^2 t^3}{3} \Gamma(4 + \alpha) \right] \sin(2\pi x) \sin(2\pi y) - t^{6+2\alpha} \sin^2(2\pi x) \sin^2(2\pi y),$$

where $\bar{\Omega} = [0, 1]^2$ and $T = 1$. The exact solution is $u(\mathbf{x}, t) = t^{3+\alpha} \sin(2\pi x) \sin(2\pi y)$. We choose $\Delta t = 1/2000$, $h = 1/10$ and $\alpha = 0.1$. Fig. 6 shows the exact solution u and the vertex values of the numerical solution u_h at $x = 0.3$ and $t = 1$ on Mesh I, which implies that the numerical solution can well approximate the exact solution even though the five schemes exhibit difference in accuracy. Tabs. 1, 2 gives some detailed results for the quadratic finite volume element schemes and quadratic finite element scheme. In Figs. 7, 8, we draw log-log plots of the L^2 errors vs. with mesh size h on Mesh I and Mesh II when $\Delta t = 1/2000$. One can see that spatial convergence orders of the QFE and QFVE-1 schemes are close to 3 for different α , while the spatial convergence order of other quadratic finite volume element schemes (QFVE-2, QFVE-3, QFVE-4) are nearly 2 and lower than that of QFVE-1, which agrees with the observations made in [49] for elliptic problems. Moreover, we calculate temporal convergence orders of these schemes in Tabs. 3, 4, and we can find the temporal convergence orders are nearly 2.

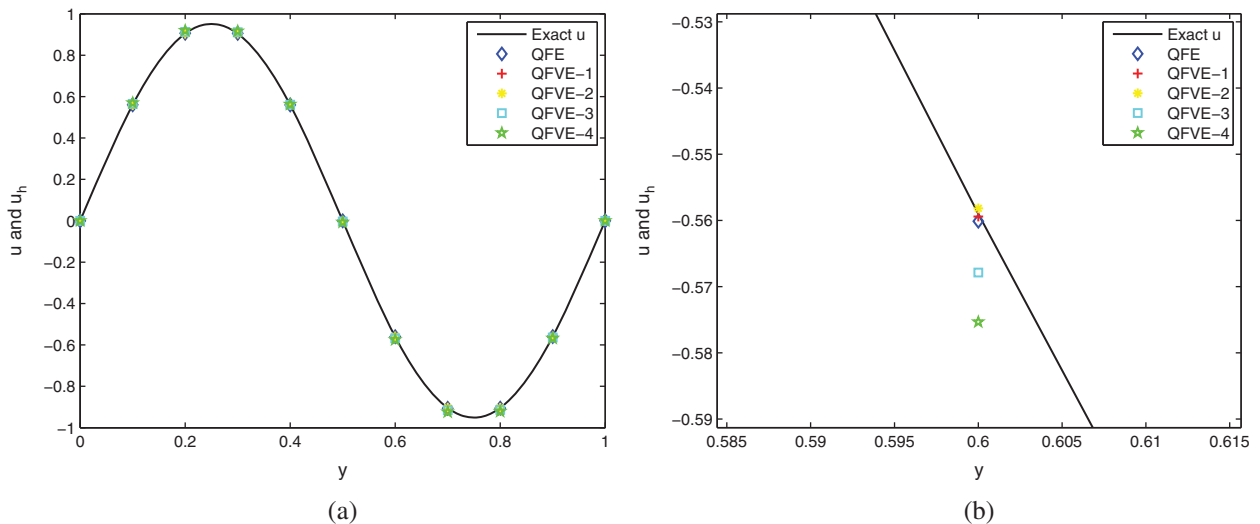


Figure 6: Comparison of the numerical solutions and the exact solution for *Example 1* on Mesh I. (a) A full profile; (b) A local enlarged profile

Table 1: Error results and spatial convergence orders with $\Delta t = 1/2000$ on Mesh I in *Example 1*

| Scheme | α | | $h = 1/5$ | $h = 1/10$ | $h = 1/20$ | $h = 1/40$ | $h = 1/80$ |
|--------|----------|---------|------------|------------|------------|------------|------------|
| QFE | 0.1 | E_u | 1.5374E-02 | 1.9390E-03 | 2.4358E-04 | 3.0502E-05 | 3.8152E-06 |
| | | R_u^1 | | 2.98711 | 2.99288 | 2.99738 | 2.99909 |
| | 0.2 | E_u | 1.5378E-02 | 1.9392E-03 | 2.4359E-04 | 3.0504E-05 | 3.8157E-06 |
| | | R_u^1 | | 2.98730 | 2.99296 | 2.99738 | 2.99897 |
| | 0.5 | E_u | 1.5394E-02 | 1.9400E-03 | 2.4362E-04 | 3.0507E-05 | 3.8170E-06 |
| | | R_u^1 | | 2.98824 | 2.99335 | 2.99741 | 2.99862 |
| | 0.9 | E_u | 1.5426E-02 | 1.9415E-03 | 2.4368E-04 | 3.0512E-05 | 3.8190E-06 |
| | | R_u^1 | | 2.99010 | 2.99413 | 2.99753 | 2.99810 |
| | 0.1 | E_u | 1.4782E-02 | 1.9197E-03 | 2.4302E-04 | 3.0486E-05 | 3.8147E-06 |
| | | R_u^1 | | 2.94484 | 2.98177 | 2.99483 | 2.99850 |
| QFVE-1 | 0.2 | E_u | 1.4783E-02 | 1.9198E-03 | 2.4302E-04 | 3.0487E-05 | 3.8150E-06 |
| | | R_u^1 | | 2.94493 | 2.98180 | 2.99482 | 2.99841 |
| | 0.5 | E_u | 1.4790E-02 | 1.9201E-03 | 2.4303E-04 | 3.0489E-05 | 3.8160E-06 |
| | | R_u^1 | | 2.94537 | 2.98196 | 2.99480 | 2.99815 |
| | 0.9 | E_u | 1.4805E-02 | 1.9208E-03 | 2.4306E-04 | 3.0492E-05 | 3.8175E-06 |
| | | R_u^1 | | 2.94633 | 2.98230 | 2.99483 | 2.99772 |
| | 0.1 | E_u | 1.6242E-02 | 2.2118E-03 | 3.1919E-04 | 5.5340E-05 | 1.1798E-05 |
| | | R_u^1 | | 2.87640 | 2.79275 | 2.52803 | 2.22973 |
| | 0.2 | E_u | 1.6244E-02 | 2.2123E-03 | 3.1933E-04 | 5.5389E-05 | 1.1819E-05 |
| | | R_u^1 | | 2.87633 | 2.79243 | 2.52736 | 2.22850 |
| QFVE-2 | 0.5 | E_u | 1.6257E-02 | 2.2142E-03 | 3.1986E-04 | 5.5573E-05 | 1.1889E-05 |
| | | R_u^1 | | 2.87615 | 2.79128 | 2.52500 | 2.22480 |
| | 0.9 | E_u | 1.6281E-02 | 2.2177E-03 | 3.2077E-04 | 5.5874E-05 | 1.1996E-05 |
| | | R_u^1 | | 2.87601 | 2.78944 | 2.52131 | 2.21962 |
| | 0.1 | E_u | 1.4931E-02 | 4.5874E-03 | 1.2418E-03 | 3.1723E-04 | 7.9750E-05 |
| | | R_u^1 | | 1.70251 | 1.88525 | 1.96884 | 1.99197 |
| | 0.2 | E_u | 1.4945E-02 | 4.5932E-03 | 1.2434E-03 | 3.1762E-04 | 7.9841E-05 |
| | | R_u^1 | | 1.70211 | 1.88524 | 1.96887 | 1.99209 |
| | 0.5 | E_u | 1.4998E-02 | 4.6150E-03 | 1.2494E-03 | 3.1914E-04 | 8.0206E-05 |
| | | R_u^1 | | 1.70039 | 1.88511 | 1.96894 | 1.99242 |
| QFVE-3 | 0.9 | E_u | 1.5081E-02 | 4.6506E-03 | 1.2593E-03 | 3.2168E-04 | 8.0821E-05 |
| | | R_u^1 | | 1.69725 | 1.88475 | 1.96897 | 1.99283 |
| | 0.1 | E_u | 3.2294E-02 | 9.3096E-03 | 2.4168E-03 | 6.0999E-04 | 1.5287E-04 |
| | | R_u^1 | | 1.79448 | 1.94560 | 1.98626 | 1.99652 |
| | 0.2 | E_u | 3.2345E-02 | 9.3225E-03 | 2.4200E-03 | 6.1079E-04 | 1.5306E-04 |
| | | R_u^1 | | 1.79477 | 1.94567 | 1.98629 | 1.99659 |
| | 0.5 | E_u | 3.2537E-02 | 9.3717E-03 | 2.4324E-03 | 6.1387E-04 | 1.5381E-04 |
| | | R_u^1 | | 1.79568 | 1.94592 | 1.98639 | 1.99678 |
| | 0.9 | E_u | 3.2842E-02 | 9.4524E-03 | 2.4529E-03 | 6.1897E-04 | 1.5506E-04 |
| | | R_u^1 | | 1.79681 | 1.94622 | 1.98652 | 1.99701 |

Table 2: Error results and spatial convergence orders with $\Delta t = 1/2000$ on Mesh II in *Example 1*

| Scheme | α | | $h = 1/5$ | $h = 1/10$ | $h = 1/20$ | $h = 1/40$ | $h = 1/80$ |
|--------|----------|---------|------------|------------|------------|------------|------------|
| QFE | 0.1 | E_u | 1.6991E-02 | 2.1497E-03 | 2.6744E-04 | 3.3367E-05 | 4.1695E-06 |
| | | R_u^1 | 2.98255 | 3.00683 | 3.00271 | 3.00050 | |
| | 0.2 | E_u | 1.6996E-02 | 2.1499E-03 | 2.6745E-04 | 3.3369E-05 | 4.1700E-06 |
| | | R_u^1 | 2.98284 | 3.00691 | 3.00270 | 3.00039 | |
| | 0.5 | E_u | 1.7016E-02 | 2.1507E-03 | 2.6748E-04 | 3.3372E-05 | 4.1713E-06 |
| | | R_u^1 | 2.98402 | 3.00728 | 3.00274 | 3.00007 | |
| | 0.9 | E_u | 1.7054E-02 | 2.1524E-03 | 2.6755E-04 | 3.3377E-05 | 4.1733E-06 |
| | | R_u^1 | 2.98605 | 3.00806 | 3.00288 | 2.99959 | |
| QFVE-1 | 0.1 | E_u | 1.6436E-02 | 2.1287E-03 | 2.6697E-04 | 3.3367E-05 | 4.1703E-06 |
| | | R_u^1 | 2.94882 | 2.99519 | 3.00019 | 3.00021 | |
| | 0.2 | E_u | 1.6439E-02 | 2.1288E-03 | 2.6698E-04 | 3.3368E-05 | 4.1706E-06 |
| | | R_u^1 | 2.94907 | 2.99524 | 3.00018 | 3.00012 | |
| | 0.5 | E_u | 1.6454E-02 | 2.1292E-03 | 2.6699E-04 | 3.3370E-05 | 4.1716E-06 |
| | | R_u^1 | 2.95000 | 2.99544 | 3.00018 | 2.99988 | |
| | 0.9 | E_u | 1.6477E-02 | 2.1301E-03 | 2.6703E-04 | 3.3373E-05 | 4.1732E-06 |
| | | R_u^1 | 2.95148 | 2.99585 | 3.00023 | 2.99948 | |
| QFVE-2 | 0.1 | E_u | 1.7951E-02 | 2.4431E-03 | 3.4969E-04 | 6.0279E-05 | 1.2808E-05 |
| | | R_u^1 | 2.87733 | 2.80453 | 2.53636 | 2.23464 | |
| | 0.2 | E_u | 1.7957E-02 | 2.4438E-03 | 3.4989E-04 | 6.0346E-05 | 1.2833E-05 |
| | | R_u^1 | 2.87741 | 2.80415 | 2.53556 | 2.23336 | |
| | 0.5 | E_u | 1.7981E-02 | 2.4465E-03 | 3.5063E-04 | 6.0592E-05 | 1.2921E-05 |
| | | R_u^1 | 2.87764 | 2.80273 | 2.53273 | 2.22942 | |
| | 0.9 | E_u | 1.8019E-02 | 2.4513E-03 | 3.5186E-04 | 6.0990E-05 | 1.3055E-05 |
| | | R_u^1 | 2.87792 | 2.80051 | 2.52835 | 2.22391 | |
| QFVE-3 | 0.1 | E_u | 1.6936E-02 | 4.9637E-03 | 1.3456E-03 | 3.4475E-04 | 8.6783E-05 |
| | | R_u^1 | 1.77061 | 1.88317 | 1.96464 | 1.99006 | |
| | 0.2 | E_u | 1.6954E-02 | 4.9713E-03 | 1.3477E-03 | 3.4527E-04 | 8.6907E-05 |
| | | R_u^1 | 1.76990 | 1.88316 | 1.96467 | 1.99018 | |
| | 0.5 | E_u | 1.7019E-02 | 4.9998E-03 | 1.3555E-03 | 3.4727E-04 | 8.7391E-05 |
| | | R_u^1 | 1.76720 | 1.88302 | 1.96475 | 1.99049 | |
| | 0.9 | E_u | 1.7124E-02 | 5.0457E-03 | 1.3683E-03 | 3.5053E-04 | 8.8189E-05 |
| | | R_u^1 | 1.76284 | 1.88265 | 1.96481 | 1.99086 | |
| QFVE-4 | 0.1 | E_u | 3.5054E-02 | 1.0067E-02 | 2.6271E-03 | 6.6460E-04 | 1.6671E-04 |
| | | R_u^1 | 1.79998 | 1.93807 | 1.98289 | 1.99513 | |
| | 0.2 | E_u | 3.5115E-02 | 1.0083E-02 | 2.6312E-03 | 6.6563E-04 | 1.6696E-04 |
| | | R_u^1 | 1.80014 | 1.93816 | 1.98292 | 1.99519 | |
| | 0.5 | E_u | 3.5345E-02 | 1.0145E-02 | 2.6469E-03 | 6.6956E-04 | 1.6793E-04 |
| | | R_u^1 | 1.80067 | 1.93845 | 1.98303 | 1.99537 | |
| | 0.9 | E_u | 3.5715E-02 | 1.0247E-02 | 2.6726E-03 | 6.7598E-04 | 1.6951E-04 |
| | | R_u^1 | 1.80139 | 1.93883 | 1.98318 | 1.99558 | |

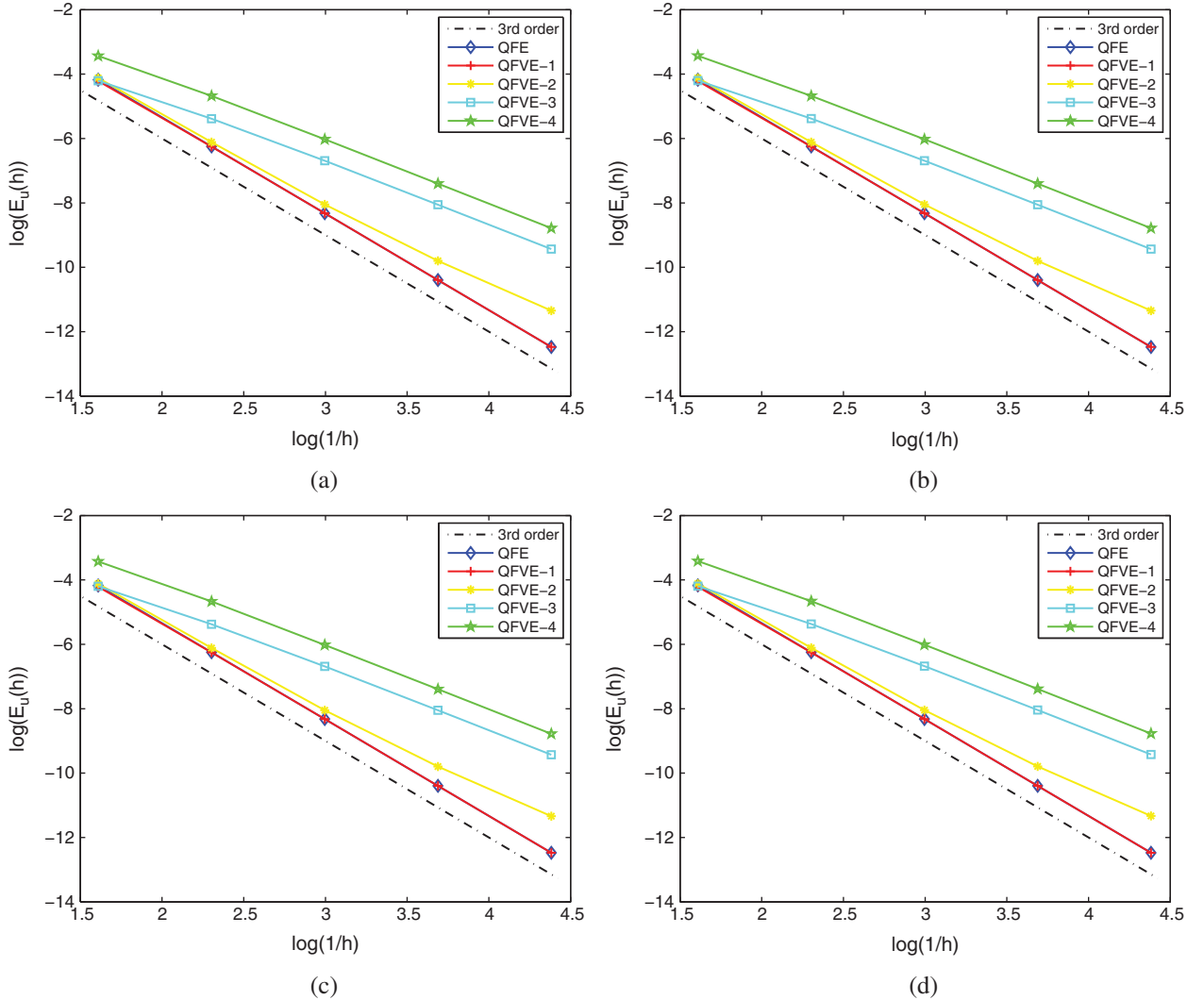


Figure 7: L^2 errors of the numerical solution on Mesh I in *Example 1*. (a) $\alpha = 0.1$; (b) $\alpha = 0.2$; (c) $\alpha = 0.5$; (d) $\alpha = 0.9$

3.2 Example 2

Solve Eqs. (1)–(3) with $\bar{\Omega} = [0, 2]^2$, $T = 2$, $f(u) = \sin(u)$ and

$$g(\mathbf{x}, t) = 3t^2 g_1(\mathbf{x}) - 12 \left[t^3 + \frac{6t^{3-\alpha}}{\Gamma(4-\alpha)} \right] g_2(\mathbf{x}) - \sin(t^3 g_1(\mathbf{x})),$$

where

$$g_1(\mathbf{x}) = x(x-0.5)(x-1.5)(x-2)y(y-0.5)(y-1.5)(y-2),$$

$$g_2(\mathbf{x}) = x(x-0.5)(x-1.5)(x-2) \left(y^2 - 2y + \frac{19}{24} \right) + y(y-0.5)(y-1.5)(y-2) \left(x^2 - 2x + \frac{19}{24} \right).$$

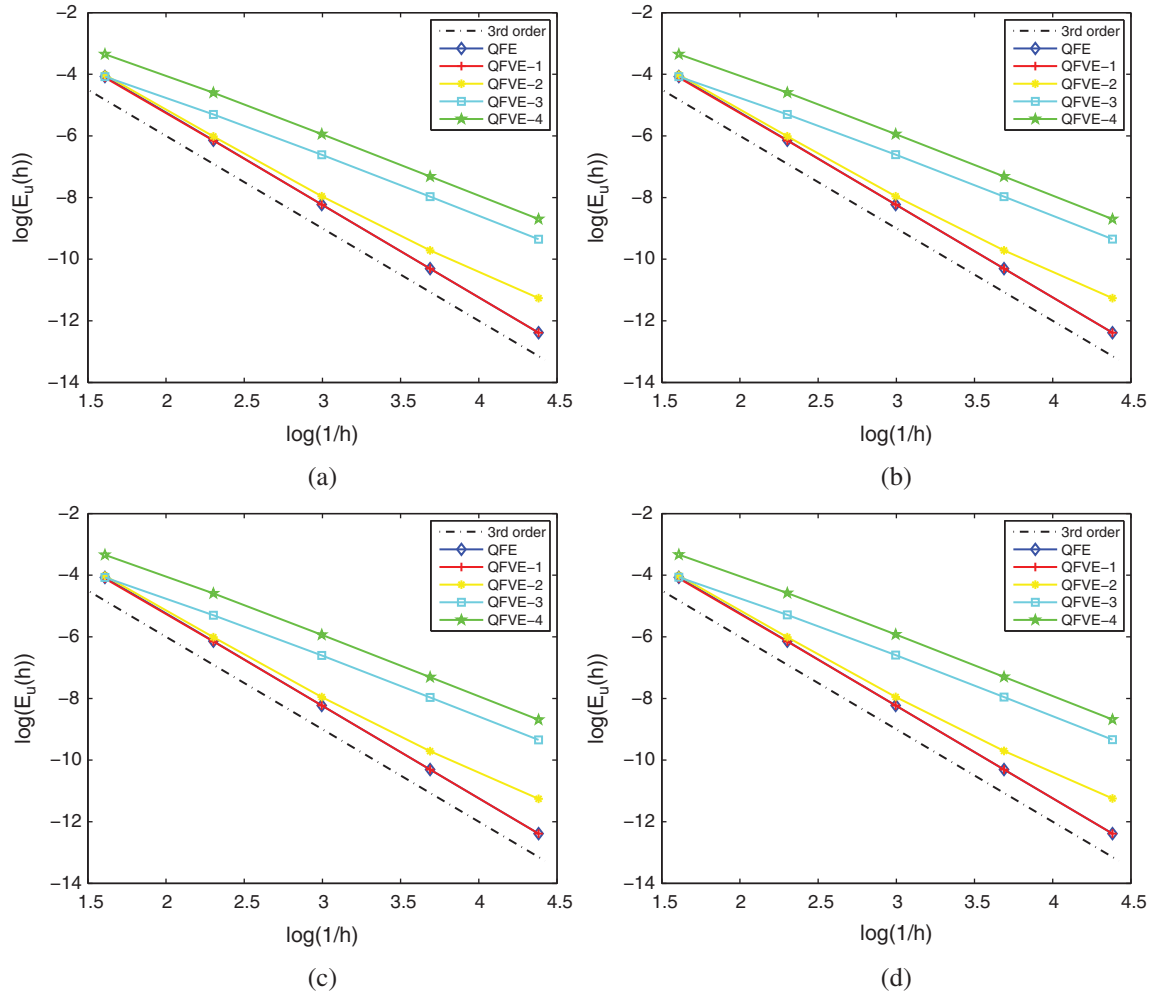


Figure 8: L^2 errors of the numerical solution on Mesh II in *Example 1*. (a) $\alpha = 0.1$; (b) $\alpha = 0.2$; (c) $\alpha = 0.5$; (d) $\alpha = 0.9$

The exact solution to this example is:

$$u(\mathbf{x}, t) = t^3 x(x - 0.5)(x - 1.5)(x - 2)y(y - 0.5)(y - 1.5)(y - 2).$$

Analogously, we calculate the L^2 errors and spatial convergence orders for several kinds of quadratic finite volume element schemes and quadratic finite element scheme, see Tabs. 5, 6. The convergence behavior is similar to that for *Example 1*. Moreover, when $\alpha = 0.1, 0.2, 0.5, 0.9$ we draw the log–log plots for these five schemes on Mesh II, and find that the converge orders don't change with α , see Fig. 9.

3.3 Example 3

We take the space-time domain $\bar{\Omega} \times [0, T] = [0, 1]^2 \times [0, 1]$, the nonlinear term $f(u) = u^3 - u$ and the source term

$$g(\mathbf{x}, t) = \left[2e^t + 8\pi^2 e^t + 8\pi^2 t^{1-\alpha} E_{1, 2-\alpha}(t) \right] \sin(2\pi x) \sin(2\pi y) - e^{3t} \sin^3(2\pi x) \sin^3(2\pi y),$$

Table 3: Error results and temporal convergence orders with $h = 1/160$ on Mesh I in *Example 1*

| Scheme | α | | $\Delta t = 1/4$ | $\Delta t = 1/8$ | $\Delta t = 1/16$ | $\Delta t = 1/32$ |
|--------|----------|---------|------------------|------------------|-------------------|-------------------|
| QFE | 0.1 | E_u | 3.7630E-03 | 1.4679E-03 | 4.6863E-04 | 1.3264E-04 |
| | | R_u^2 | | 1.35809 | 1.64726 | 1.82090 |
| | 0.2 | E_u | 5.2654E-03 | 1.6715E-03 | 4.9435E-04 | 1.3573E-04 |
| | | R_u^2 | | 1.65542 | 1.75752 | 1.86482 |
| | 0.5 | E_u | 1.2032E-02 | 3.0704E-03 | 7.7387E-04 | 1.9313E-04 |
| | | R_u^2 | | 1.97040 | 1.98825 | 2.00251 |
| | 0.9 | E_u | 2.1267E-02 | 5.3181E-03 | 1.3141E-03 | 3.2290E-04 |
| | | R_u^2 | | 1.99964 | 2.01682 | 2.02493 |
| | 0.1 | E_u | 3.7630E-03 | 1.4679E-03 | 4.6863E-04 | 1.3264E-04 |
| | | R_u^2 | | 1.35809 | 1.64725 | 1.82091 |
| QFVE-1 | 0.2 | E_u | 5.2654E-03 | 1.6715E-03 | 4.9435E-04 | 1.3573E-04 |
| | | R_u^2 | | 1.65542 | 1.75752 | 1.86483 |
| | 0.5 | E_u | 1.2032E-02 | 3.0704E-03 | 7.7387E-04 | 1.9313E-04 |
| | | R_u^2 | | 1.97040 | 1.98825 | 2.00253 |
| | 0.9 | E_u | 2.1267E-02 | 5.3181E-03 | 1.3141E-03 | 3.2290E-04 |
| | | R_u^2 | | 1.99964 | 2.01683 | 2.02494 |
| | 0.1 | E_u | 3.7637E-03 | 1.4681E-03 | 4.6863E-04 | 1.3258E-04 |
| | | R_u^2 | | 1.35817 | 1.64744 | 1.82161 |
| | 0.2 | E_u | 5.2671E-03 | 1.6726E-03 | 4.9519E-04 | 1.3642E-04 |
| | | R_u^2 | | 1.65489 | 1.75607 | 1.85989 |
| QFVE-2 | 0.5 | E_u | 1.2035E-02 | 3.0756E-03 | 7.7601E-04 | 1.9518E-04 |
| | | R_u^2 | | 1.96962 | 1.98534 | 1.99130 |
| | 0.9 | E_u | 2.1269E-02 | 5.3206E-03 | 1.3166E-03 | 3.2538E-04 |
| | | R_u^2 | | 1.99913 | 2.01477 | 2.01663 |
| | 0.1 | E_u | 3.7592E-03 | 1.4679E-03 | 4.7026E-04 | 1.3592E-04 |
| | | R_u^2 | | 1.35667 | 1.64220 | 1.79072 |
| | 0.2 | E_u | 5.2539E-03 | 1.6643E-03 | 4.8986E-04 | 1.3350E-04 |
| | | R_u^2 | | 1.65845 | 1.76449 | 1.87549 |
| | 0.5 | E_u | 1.2016E-02 | 3.0549E-03 | 7.5950E-04 | 1.7996E-04 |
| | | R_u^2 | | 1.97572 | 2.00801 | 2.07741 |
| QFVE-3 | 0.9 | E_u | 2.1250E-02 | 5.3007E-03 | 1.2968E-03 | 3.0587E-04 |
| | | R_u^2 | | 2.00320 | 2.03119 | 2.08398 |
| | 0.1 | E_u | 3.7566E-03 | 1.4689E-03 | 4.7334E-04 | 1.4214E-04 |
| | | R_u^2 | | 1.35466 | 1.63384 | 1.73558 |
| | 0.2 | E_u | 5.2442E-03 | 1.6589E-03 | 4.8737E-04 | 1.3499E-04 |
| | | R_u^2 | | 1.66054 | 1.76712 | 1.85212 |
| | 0.5 | E_u | 1.2001E-02 | 3.0415E-03 | 7.4735E-04 | 1.6998E-04 |
| | | R_u^2 | | 1.98033 | 2.02493 | 2.13638 |
| | 0.9 | E_u | 2.1235E-02 | 5.2854E-03 | 1.2817E-03 | 2.9133E-04 |
| | | R_u^2 | | 2.00635 | 2.04395 | 2.13736 |

Table 4: Error results and temporal convergence orders with $h = 1/160$ on Mesh II in *Example 1*

| Scheme | α | | $\Delta t = 1/4$ | $\Delta t = 1/8$ | $\Delta t = 1/16$ | $\Delta t = 1/32$ |
|--------|----------|---------|------------------|------------------|-------------------|-------------------|
| QFE | 0.1 | E_u | 3.7630E-03 | 1.4679E-03 | 4.6863E-04 | 1.3264E-04 |
| | | R_u^2 | | 1.35809 | 1.64726 | 1.82090 |
| | 0.2 | E_u | 5.2654E-03 | 1.6715E-03 | 4.9435E-04 | 1.3573E-04 |
| | | R_u^2 | | 1.65541 | 1.75752 | 1.86482 |
| | 0.5 | E_u | 1.2032E-02 | 3.0704E-03 | 7.7388E-04 | 1.9313E-04 |
| | | R_u^2 | | 1.97040 | 1.98825 | 2.00250 |
| | 0.9 | E_u | 2.1267E-02 | 5.3181E-03 | 1.3141E-03 | 3.2290E-04 |
| | | R_u^2 | | 1.99964 | 2.01682 | 2.02492 |
| | 0.1 | E_u | 3.7630E-03 | 1.4679E-03 | 4.6863E-04 | 1.3264E-04 |
| | | R_u^2 | | 1.35809 | 1.64726 | 1.82091 |
| QFVE-1 | 0.2 | E_u | 5.2654E-03 | 1.6715E-03 | 4.9435E-04 | 1.3573E-04 |
| | | R_u^2 | | 1.65542 | 1.75752 | 1.86483 |
| | 0.5 | E_u | 1.2032E-02 | 3.0704E-03 | 7.7387E-04 | 1.9313E-04 |
| | | R_u^2 | | 1.97040 | 1.98825 | 2.00252 |
| | 0.9 | E_u | 2.1267E-02 | 5.3181E-03 | 1.3141E-03 | 3.2290E-04 |
| | | R_u^2 | | 1.99964 | 2.01683 | 2.02493 |
| | 0.1 | E_u | 3.7634E-03 | 1.4678E-03 | 4.6827E-04 | 1.3222E-04 |
| | | R_u^2 | | 1.35839 | 1.64821 | 1.82445 |
| | 0.2 | E_u | 5.2670E-03 | 1.6724E-03 | 4.9492E-04 | 1.3614E-04 |
| | | R_u^2 | | 1.65505 | 1.75667 | 1.86215 |
| QFVE-2 | 0.5 | E_u | 1.2035E-02 | 3.0726E-03 | 7.7596E-04 | 1.9511E-04 |
| | | R_u^2 | | 1.96963 | 1.98542 | 1.99170 |
| | 0.9 | E_u | 2.1270E-02 | 5.3207E-03 | 1.3167E-03 | 3.2544E-04 |
| | | R_u^2 | | 1.99911 | 2.01472 | 2.01643 |
| | 0.1 | E_u | 3.7608E-03 | 1.4700E-03 | 4.7249E-04 | 1.3833E-04 |
| | | R_u^2 | | 1.35529 | 1.63741 | 1.77221 |
| | 0.2 | E_u | 5.2545E-03 | 1.6656E-03 | 4.9154E-04 | 1.3552E-04 |
| | | R_u^2 | | 1.65748 | 1.76069 | 1.85881 |
| | 0.5 | E_u | 1.2015E-02 | 3.0548E-03 | 7.5967E-04 | 1.8046E-04 |
| | | R_u^2 | | 1.97572 | 2.00764 | 2.07370 |
| QFVE-3 | 0.9 | E_u | 2.1249E-02 | 5.3001E-03 | 1.2963E-03 | 3.0543E-04 |
| | | R_u^2 | | 2.00332 | 2.03165 | 2.08546 |
| | 0.1 | E_u | 3.7596E-03 | 1.4726E-03 | 4.7739E-04 | 1.4668E-04 |
| | | R_u^2 | | 1.35219 | 1.62516 | 1.70246 |
| | 0.2 | E_u | 5.2453E-03 | 1.6612E-03 | 4.9042E-04 | 1.3897E-04 |
| | | R_u^2 | | 1.65882 | 1.76009 | 1.81921 |
| | 0.5 | E_u | 1.2000E-02 | 3.0412E-03 | 7.4760E-04 | 1.7120E-04 |
| | | R_u^2 | | 1.98038 | 2.02429 | 2.12658 |
| | 0.9 | E_u | 2.1233E-02 | 5.2841E-03 | 1.2806E-03 | 2.9057E-04 |
| | | R_u^2 | | 2.00660 | 2.04486 | 2.13982 |

Table 5: Error results and spatial convergence orders with $\Delta t = 1/2000$ on Mesh I in *Example 2*

| Scheme | α | | $h = 1/5$ | $h = 1/10$ | $h = 1/20$ | $h = 1/40$ | $h = 1/80$ |
|--------|----------|---------|------------|------------|------------|------------|------------|
| QFE | 0.1 | E_u | 3.4789E-02 | 4.4415E-03 | 5.3823E-04 | 6.6439E-05 | 8.2777E-06 |
| | | R_u^1 | | 2.96951 | 3.04474 | 3.01812 | 3.00474 |
| | 0.2 | E_u | 3.4787E-02 | 4.4414E-03 | 5.3823E-04 | 6.6440E-05 | 8.2779E-06 |
| | | R_u^1 | | 2.96947 | 3.04472 | 3.01811 | 3.00471 |
| | 0.5 | E_u | 3.4783E-02 | 4.4412E-03 | 5.3822E-04 | 6.6440E-05 | 8.2784E-06 |
| | | R_u^1 | | 2.96936 | 3.04466 | 3.01807 | 3.00463 |
| | 0.9 | E_u | 3.4778E-02 | 4.4409E-03 | 5.3821E-04 | 6.6441E-05 | 8.2790E-06 |
| | | R_u^1 | | 2.96924 | 3.04460 | 3.01803 | 3.00455 |
| | 0.1 | E_u | 3.1871E-02 | 4.2336E-03 | 5.2968E-04 | 6.6155E-05 | 8.2687E-06 |
| | | R_u^1 | | 2.91229 | 2.99871 | 3.00120 | 3.00011 |
| QFVE-1 | 0.2 | E_u | 3.1870E-02 | 4.2336E-03 | 5.2968E-04 | 6.6155E-05 | 8.2689E-06 |
| | | R_u^1 | | 2.91226 | 2.99870 | 3.00119 | 3.00008 |
| | 0.5 | E_u | 3.1867E-02 | 4.2335E-03 | 5.2967E-04 | 6.6156E-05 | 8.2693E-06 |
| | | R_u^1 | | 2.91217 | 2.99866 | 3.00116 | 3.00002 |
| | 0.9 | E_u | 3.1864E-02 | 4.2333E-03 | 5.2967E-04 | 6.6156E-05 | 8.2698E-06 |
| | | R_u^1 | | 2.91208 | 2.99862 | 3.00114 | 2.99996 |
| | 0.1 | E_u | 3.2196E-02 | 4.4497E-03 | 6.0169E-04 | 9.2053E-05 | 1.7519E-05 |
| | | R_u^1 | | 2.85511 | 2.88661 | 2.70849 | 2.39355 |
| | 0.2 | E_u | 3.2195E-02 | 4.4495E-03 | 6.0166E-04 | 9.2044E-05 | 1.7518E-05 |
| | | R_u^1 | | 2.85510 | 2.88664 | 2.70855 | 2.39348 |
| QFVE-2 | 0.5 | E_u | 3.2192E-02 | 4.4492E-03 | 6.0158E-04 | 9.2019E-05 | 1.7515E-05 |
| | | R_u^1 | | 2.85507 | 2.88672 | 2.70874 | 2.39335 |
| | 0.9 | E_u | 3.2188E-02 | 4.4488E-03 | 6.0151E-04 | 9.2003E-05 | 1.7515E-05 |
| | | R_u^1 | | 2.85503 | 2.88676 | 2.70884 | 2.39313 |
| | 0.1 | E_u | 3.2437E-02 | 6.5414E-03 | 1.6402E-03 | 4.1559E-04 | 1.0435E-04 |
| | | R_u^1 | | 2.31000 | 1.99569 | 1.98067 | 1.99368 |
| | 0.2 | E_u | 3.2435E-02 | 6.5403E-03 | 1.6399E-03 | 4.1549E-04 | 1.0433E-04 |
| | | R_u^1 | | 2.31013 | 1.99576 | 1.98070 | 1.99372 |
| | 0.5 | E_u | 3.2428E-02 | 6.5373E-03 | 1.6389E-03 | 4.1523E-04 | 1.0425E-04 |
| | | R_u^1 | | 2.31047 | 1.99596 | 1.98076 | 1.99380 |
| QFVE-3 | 0.9 | E_u | 3.2424E-02 | 6.5353E-03 | 1.6382E-03 | 4.1503E-04 | 1.0420E-04 |
| | | R_u^1 | | 2.31071 | 1.99617 | 1.98083 | 1.99389 |
| | 0.1 | E_u | 4.3651E-02 | 1.2090E-02 | 3.1313E-03 | 7.9062E-04 | 1.9815E-04 |
| | | R_u^1 | | 1.85224 | 1.94895 | 1.98570 | 1.99636 |
| | 0.2 | E_u | 4.3644E-02 | 1.2087E-02 | 3.1306E-03 | 7.9044E-04 | 1.9811E-04 |
| | | R_u^1 | | 1.85229 | 1.94896 | 1.98571 | 1.99637 |
| | 0.5 | E_u | 4.3624E-02 | 1.2080E-02 | 3.1288E-03 | 7.8997E-04 | 1.9798E-04 |
| | | R_u^1 | | 1.85246 | 1.94901 | 1.98573 | 1.99642 |
| | 0.9 | E_u | 4.3611E-02 | 1.2075E-02 | 3.1273E-03 | 7.8958E-04 | 1.9788E-04 |
| | | R_u^1 | | 1.85266 | 1.94907 | 1.98575 | 1.99646 |

Table 6: Error results and spatial convergence orders with $\Delta t = 1/2000$ on Mesh II in *Example 2*

| Scheme | α | | $h = 1/5$ | $h = 1/10$ | $h = 1/20$ | $h = 1/40$ | $h = 1/80$ |
|--------|----------|---------|------------|------------|------------|------------|------------|
| QFE | 0.1 | E_u | 3.8651E-02 | 4.9359E-03 | 5.9810E-04 | 7.3868E-05 | 9.2054E-06 |
| | | R_u^1 | | 2.96912 | 3.04487 | 3.01736 | 3.00441 |
| | 0.2 | E_u | 3.8649E-02 | 4.9358E-03 | 5.9810E-04 | 7.3869E-05 | 9.2056E-06 |
| | | R_u^1 | | 2.96908 | 3.04485 | 3.01735 | 3.00438 |
| | 0.5 | E_u | 3.8644E-02 | 4.9356E-03 | 5.9809E-04 | 7.3869E-05 | 9.2061E-06 |
| | | R_u^1 | | 2.96897 | 3.04479 | 3.01731 | 3.00431 |
| | 0.9 | E_u | 3.8639E-02 | 4.9353E-03 | 5.9808E-04 | 7.3870E-05 | 9.2066E-06 |
| | | R_u^1 | | 2.96886 | 3.04472 | 3.01728 | 3.00424 |
| QFVE-1 | 0.1 | E_u | 3.5708E-02 | 4.7460E-03 | 5.9083E-04 | 7.3656E-05 | 9.2005E-06 |
| | | R_u^1 | | 2.91146 | 3.00588 | 3.00388 | 3.00102 |
| | 0.2 | E_u | 3.5707E-02 | 4.7459E-03 | 5.9083E-04 | 7.3656E-05 | 9.2007E-06 |
| | | R_u^1 | | 2.91143 | 3.00586 | 3.00387 | 3.00100 |
| | 0.5 | E_u | 3.5703E-02 | 4.7457E-03 | 5.9083E-04 | 7.3657E-05 | 9.2011E-06 |
| | | R_u^1 | | 2.91135 | 3.00582 | 3.00385 | 3.00095 |
| | 0.9 | E_u | 3.5700E-02 | 4.7456E-03 | 5.9082E-04 | 7.3657E-05 | 9.2015E-06 |
| | | R_u^1 | | 2.91126 | 3.00578 | 3.00382 | 3.00089 |
| QFVE-2 | 0.1 | E_u | 3.6034E-02 | 4.9651E-03 | 6.6231E-04 | 9.9276E-05 | 1.8465E-05 |
| | | R_u^1 | | 2.85945 | 2.90625 | 2.73799 | 2.42662 |
| | 0.2 | E_u | 3.6032E-02 | 4.9650E-03 | 6.6228E-04 | 9.9267E-05 | 1.8464E-05 |
| | | R_u^1 | | 2.85943 | 2.90628 | 2.73805 | 2.42657 |
| | 0.5 | E_u | 3.6028E-02 | 4.9646E-03 | 6.6219E-04 | 9.9241E-05 | 1.8460E-05 |
| | | R_u^1 | | 2.85940 | 2.90635 | 2.73824 | 2.42649 |
| | 0.9 | E_u | 3.6024E-02 | 4.9642E-03 | 6.6212E-04 | 9.9224E-05 | 1.8459E-05 |
| | | R_u^1 | | 2.85935 | 2.90638 | 2.73834 | 2.42633 |
| QFVE-3 | 0.1 | E_u | 3.5687E-02 | 6.8456E-03 | 1.6915E-03 | 4.2850E-04 | 1.0767E-04 |
| | | R_u^1 | | 2.38217 | 2.01689 | 1.98093 | 1.99262 |
| | 0.2 | E_u | 3.5685E-02 | 6.8446E-03 | 1.6911E-03 | 4.2840E-04 | 1.0765E-04 |
| | | R_u^1 | | 2.38230 | 2.01697 | 1.98096 | 1.99265 |
| | 0.5 | E_u | 3.5679E-02 | 6.8417E-03 | 1.6901E-03 | 4.2813E-04 | 1.0757E-04 |
| | | R_u^1 | | 2.38265 | 2.01722 | 1.98103 | 1.99274 |
| | 0.9 | E_u | 3.5676E-02 | 6.8399E-03 | 1.6894E-03 | 4.2792E-04 | 1.0751E-04 |
| | | R_u^1 | | 2.38290 | 2.01746 | 1.98111 | 1.99282 |
| QFVE-4 | 0.1 | E_u | 4.4968E-02 | 1.2391E-02 | 3.2256E-03 | 8.1655E-04 | 2.0488E-04 |
| | | R_u^1 | | 1.85956 | 1.94168 | 1.98197 | 1.99474 |
| | 0.2 | E_u | 4.4962E-02 | 1.2389E-02 | 3.2249E-03 | 8.1637E-04 | 2.0483E-04 |
| | | R_u^1 | | 1.85965 | 1.94171 | 1.98197 | 1.99476 |
| | 0.5 | E_u | 4.4946E-02 | 1.2382E-02 | 3.2231E-03 | 8.1588E-04 | 2.0471E-04 |
| | | R_u^1 | | 1.85991 | 1.94177 | 1.98200 | 1.99480 |
| | 0.9 | E_u | 4.4936E-02 | 1.2377E-02 | 3.2215E-03 | 8.1548E-04 | 2.0460E-04 |
| | | R_u^1 | | 1.86020 | 1.94185 | 1.98202 | 1.99484 |

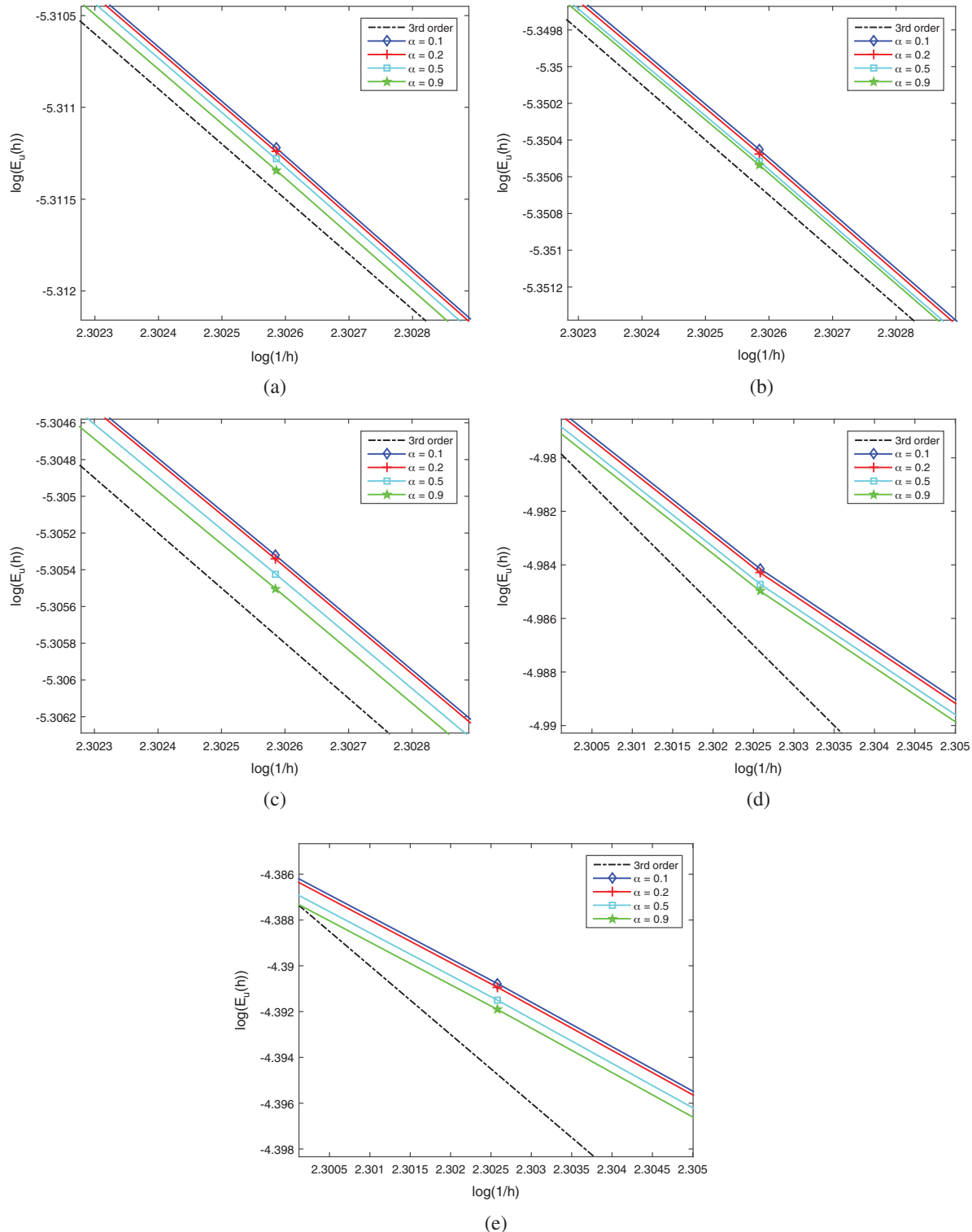


Figure 9: L^2 errors of the numerical solution on Mesh II in *Example 2*. (a) QFE; (b) QFVE-1; (c) QFVE-2; (d) QFVE-3; (e) QFVE-4

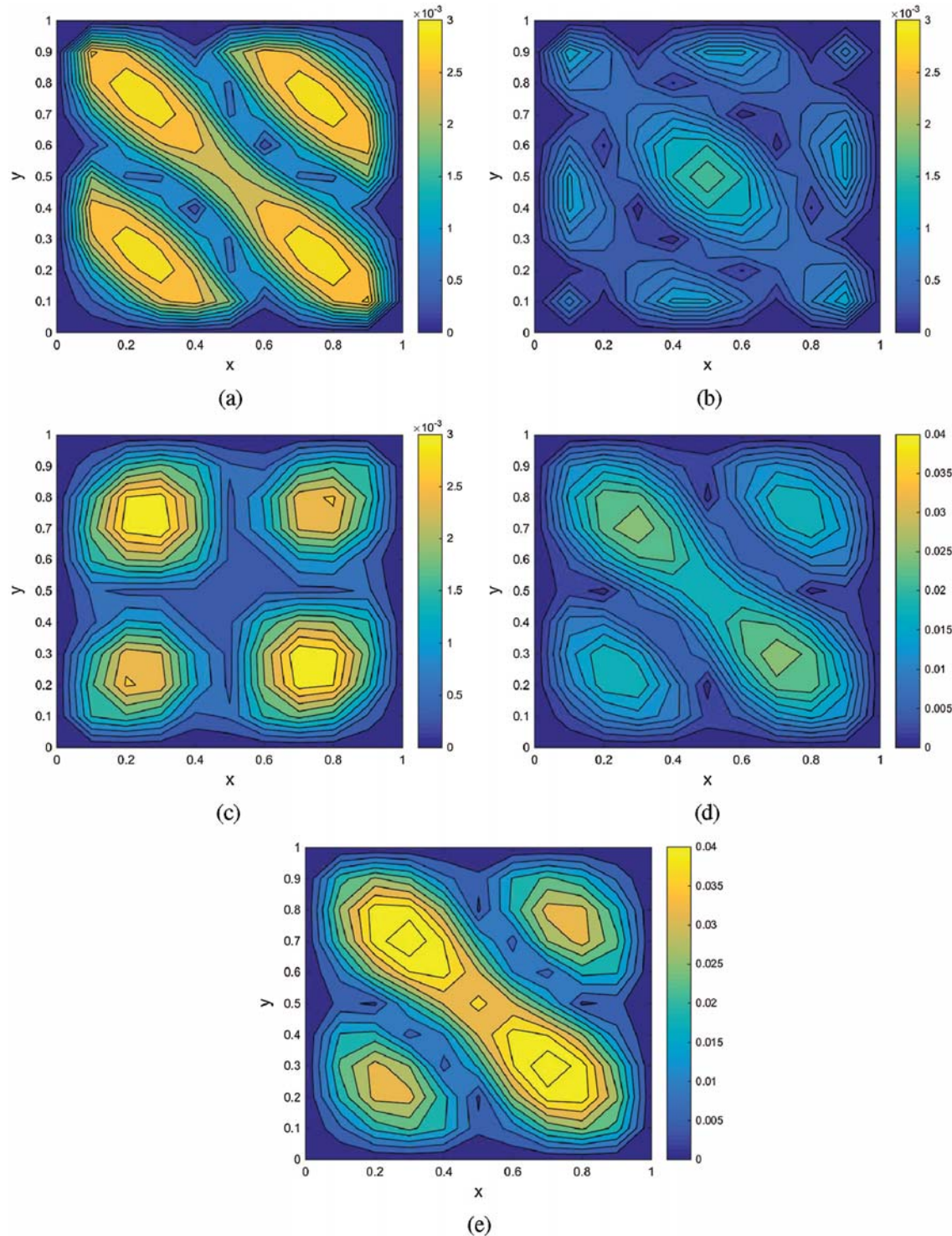


Figure 10: Contour plots of $|u - u_h|$ on Mesh I in *Example 3*. (a) QFE; (b) QFVE-1; (c) QFVE-2; (d) QFVE-3; (e) QFVE-4

Table 7: Numerical results with $\Delta t = 1/2000$ on Mesh I in *Example 3*

| Scheme | α | | $h = 1/5$ | $h = 1/10$ | $h = 1/20$ | $h = 1/40$ | $h = 1/80$ |
|--------|----------|---------|------------|------------|------------|------------|------------|
| QFE | 0.1 | E_u | 4.1481E-02 | 5.2684E-03 | 6.6217E-04 | 8.2923E-05 | 1.0374E-05 |
| | | R_u^1 | | 2.97701 | 2.99209 | 2.99736 | 2.99886 |
| | 0.2 | E_u | 4.1468E-02 | 5.2674E-03 | 6.6213E-04 | 8.2921E-05 | 1.0373E-05 |
| | | R_u^1 | | 2.97684 | 2.99190 | 2.99730 | 2.99888 |
| | 0.5 | E_u | 4.1435E-02 | 5.2646E-03 | 6.6202E-04 | 8.2916E-05 | 1.0372E-05 |
| | | R_u^1 | | 2.97645 | 2.99139 | 2.99715 | 2.99892 |
| | 0.9 | E_u | 4.1399E-02 | 5.2615E-03 | 6.6189E-04 | 8.2911E-05 | 1.0371E-05 |
| | | R_u^1 | | 2.97605 | 2.99081 | 2.99697 | 2.99894 |
| | 0.1 | E_u | 4.0345E-02 | 5.2291E-03 | 6.6100E-04 | 8.2887E-05 | 1.0372E-05 |
| | | R_u^1 | | 2.94777 | 2.98383 | 2.99544 | 2.99851 |
| QFVE-1 | 0.2 | E_u | 4.0330E-02 | 5.2283E-03 | 6.6097E-04 | 8.2886E-05 | 1.0371E-05 |
| | | R_u^1 | | 2.94743 | 2.98367 | 2.99540 | 2.99852 |
| | 0.5 | E_u | 4.0287E-02 | 5.2261E-03 | 6.6089E-04 | 8.2882E-05 | 1.0371E-05 |
| | | R_u^1 | | 2.94649 | 2.98325 | 2.99528 | 2.99856 |
| | 0.9 | E_u | 4.0237E-02 | 5.2236E-03 | 6.6080E-04 | 8.2878E-05 | 1.0370E-05 |
| | | R_u^1 | | 2.94542 | 2.98276 | 2.99515 | 2.99858 |
| | 0.1 | E_u | 4.3777E-02 | 5.9077E-03 | 8.3507E-04 | 1.4007E-04 | 2.9171E-05 |
| | | R_u^1 | | 2.88949 | 2.82263 | 2.57578 | 2.26351 |
| | 0.2 | E_u | 4.3772E-02 | 5.9086E-03 | 8.3549E-04 | 1.4021E-04 | 2.9208E-05 |
| | | R_u^1 | | 2.88911 | 2.82213 | 2.57507 | 2.26313 |
| QFVE-2 | 0.5 | E_u | 4.3761E-02 | 5.9117E-03 | 8.3684E-04 | 1.4065E-04 | 2.9327E-05 |
| | | R_u^1 | | 2.88800 | 2.82056 | 2.57281 | 2.26184 |
| | 0.9 | E_u | 4.3748E-02 | 5.9151E-03 | 8.3830E-04 | 1.4113E-04 | 2.9457E-05 |
| | | R_u^1 | | 2.88675 | 2.81887 | 2.57042 | 2.26038 |
| | 0.1 | E_u | 3.8981E-02 | 1.1306E-02 | 3.0314E-03 | 7.7277E-04 | 1.9412E-04 |
| | | R_u^1 | | 1.78570 | 1.89902 | 1.97187 | 1.99310 |
| | 0.2 | E_u | 3.8977E-02 | 1.1322E-02 | 3.0363E-03 | 7.7408E-04 | 1.9445E-04 |
| | | R_u^1 | | 1.78356 | 1.89867 | 1.97178 | 1.99306 |
| | 0.5 | E_u | 3.8977E-02 | 1.1372E-02 | 3.0521E-03 | 7.7824E-04 | 1.9552E-04 |
| | | R_u^1 | | 1.77714 | 1.89759 | 1.97153 | 1.99292 |
| QFVE-3 | 0.9 | E_u | 3.8967E-02 | 1.1425E-02 | 3.0690E-03 | 7.8269E-04 | 1.9665E-04 |
| | | R_u^1 | | 1.77006 | 1.89635 | 1.97125 | 1.99279 |
| | 0.1 | E_u | 8.0001E-02 | 2.2742E-02 | 5.8901E-03 | 1.4858E-03 | 3.7223E-04 |
| | | R_u^1 | | 1.81469 | 1.94898 | 1.98708 | 1.99694 |
| | 0.2 | E_u | 8.0055E-02 | 2.2776E-02 | 5.9000E-03 | 1.4883E-03 | 3.7288E-04 |
| | | R_u^1 | | 1.81345 | 1.94875 | 1.98702 | 1.99691 |
| | 0.5 | E_u | 8.0248E-02 | 2.2887E-02 | 5.9314E-03 | 1.4964E-03 | 3.7492E-04 |
| | | R_u^1 | | 1.80993 | 1.94811 | 1.98686 | 1.99683 |
| | 0.9 | E_u | 8.0435E-02 | 2.3005E-02 | 5.9650E-03 | 1.5051E-03 | 3.7712E-04 |
| | | R_u^1 | | 1.80590 | 1.94733 | 1.98667 | 1.99675 |

Table 8: Numerical results with $\Delta t = 1/2000$ on Mesh II in *Example 3*

| Scheme | α | | $h = 1/5$ | $h = 1/10$ | $h = 1/20$ | $h = 1/40$ | $h = 1/80$ |
|--------|----------|---------|------------|------------|------------|------------|------------|
| QFE | 0.1 | E_u | 4.5775E-02 | 5.8108E-03 | 7.2556E-04 | 9.0654E-05 | 1.1335E-05 |
| | | R_u^1 | | 2.97775 | 3.00156 | 3.00067 | 2.99964 |
| | 0.2 | E_u | 4.5752E-02 | 5.8105E-03 | 7.2556E-04 | 9.0653E-05 | 1.1334E-05 |
| | | R_u^1 | | 2.97711 | 3.00149 | 3.00066 | 2.99967 |
| | 0.5 | E_u | 4.5696E-02 | 5.8099E-03 | 7.2556E-04 | 9.0652E-05 | 1.1333E-05 |
| | | R_u^1 | | 2.97549 | 3.00134 | 3.00068 | 2.99976 |
| | 0.9 | E_u | 4.5639E-02 | 5.8094E-03 | 7.2557E-04 | 9.0652E-05 | 1.1333E-05 |
| | | R_u^1 | | 2.97381 | 3.00121 | 3.00070 | 2.99984 |
| QFVE-1 | 0.1 | E_u | 4.4883E-02 | 5.7726E-03 | 7.2486E-04 | 9.0665E-05 | 1.1336E-05 |
| | | R_u^1 | | 2.95887 | 2.99345 | 2.99908 | 2.99961 |
| | 0.2 | E_u | 4.4848E-02 | 5.7724E-03 | 7.2486E-04 | 9.0665E-05 | 1.1336E-05 |
| | | R_u^1 | | 2.95779 | 2.99339 | 2.99908 | 2.99964 |
| | 0.5 | E_u | 4.4755E-02 | 5.7720E-03 | 7.2488E-04 | 9.0666E-05 | 1.1335E-05 |
| | | R_u^1 | | 2.95492 | 2.99325 | 2.99911 | 2.99972 |
| | 0.9 | E_u | 4.4658E-02 | 5.7717E-03 | 7.2491E-04 | 9.0667E-05 | 1.1335E-05 |
| | | R_u^1 | | 2.95186 | 2.99312 | 2.99915 | 2.99979 |
| QFVE-2 | 0.1 | E_u | 4.8680E-02 | 6.5149E-03 | 9.1633E-04 | 1.5331E-04 | 3.1883E-05 |
| | | R_u^1 | | 2.90151 | 2.82980 | 2.57944 | 2.26557 |
| | 0.2 | E_u | 4.8643E-02 | 6.5161E-03 | 9.1675E-04 | 1.5344E-04 | 3.1917E-05 |
| | | R_u^1 | | 2.90016 | 2.82941 | 2.57887 | 2.26527 |
| | 0.5 | E_u | 4.8549E-02 | 6.5202E-03 | 9.1810E-04 | 1.5386E-04 | 3.2029E-05 |
| | | R_u^1 | | 2.89644 | 2.82819 | 2.57703 | 2.26419 |
| | 0.9 | E_u | 4.8447E-02 | 6.5248E-03 | 9.1956E-04 | 1.5431E-04 | 3.2148E-05 |
| | | R_u^1 | | 2.89240 | 2.82692 | 2.57511 | 2.26301 |
| QFVE-3 | 0.1 | E_u | 4.2879E-02 | 1.2323E-02 | 3.3070E-03 | 8.4521E-04 | 2.1258E-04 |
| | | R_u^1 | | 1.79895 | 1.89770 | 1.96816 | 1.99132 |
| | 0.2 | E_u | 4.2956E-02 | 1.2337E-02 | 3.3117E-03 | 8.4645E-04 | 2.1290E-04 |
| | | R_u^1 | | 1.79993 | 1.89732 | 1.96805 | 1.99127 |
| | 0.5 | E_u | 4.3189E-02 | 1.2382E-02 | 3.3265E-03 | 8.5044E-04 | 2.1392E-04 |
| | | R_u^1 | | 1.80242 | 1.89616 | 1.96773 | 1.99112 |
| | 0.9 | E_u | 4.3451E-02 | 1.2429E-02 | 3.3422E-03 | 8.5467E-04 | 2.1501E-04 |
| | | R_u^1 | | 1.80572 | 1.89482 | 1.96735 | 1.99097 |
| QFVE-4 | 0.1 | E_u | 8.5404E-02 | 2.4749E-02 | 6.4398E-03 | 1.6279E-03 | 4.0823E-04 |
| | | R_u^1 | | 1.78695 | 1.94227 | 1.98398 | 1.99559 |
| | 0.2 | E_u | 8.5576E-02 | 2.4780E-02 | 6.4492E-03 | 1.6304E-03 | 4.0885E-04 |
| | | R_u^1 | | 1.78801 | 1.94201 | 1.98390 | 1.99556 |
| | 0.5 | E_u | 8.6107E-02 | 2.4883E-02 | 6.4795E-03 | 1.6383E-03 | 4.1086E-04 |
| | | R_u^1 | | 1.79094 | 1.94123 | 1.98370 | 1.99548 |
| | 0.9 | E_u | 8.6678E-02 | 2.4991E-02 | 6.5118E-03 | 1.6467E-03 | 4.1300E-04 |
| | | R_u^1 | | 1.79424 | 1.94030 | 1.98345 | 1.99539 |

Table 9: Numerical results with $\Delta t = 1/100$ on Mesh I in *Example 4*

| Scheme | α | | $h = 1/5$ | $h = 1/10$ | $h = 1/20$ | $h = 1/40$ | $h = 1/80$ |
|--------|----------|---------|------------|------------|------------|------------|------------|
| QFE | 0.1 | E_u | 4.9259E-04 | 6.2585E-05 | 7.8691E-06 | 9.8500E-07 | 1.2318E-07 |
| | | R_u^1 | | 2.97649 | 2.99155 | 2.99801 | 2.99930 |
| | 0.2 | E_u | 5.2389E-04 | 6.6536E-05 | 8.3568E-06 | 1.0456E-06 | 1.3085E-07 |
| | | R_u^1 | | 2.97704 | 2.99312 | 2.99864 | 2.99831 |
| | 0.5 | E_u | 6.1113E-04 | 7.7927E-05 | 9.7900E-06 | 1.2247E-06 | 1.5342E-07 |
| | | R_u^1 | | 2.97128 | 2.99275 | 2.99892 | 2.99680 |
| | 0.9 | E_u | 6.5735E-04 | 8.3896E-05 | 1.0542E-05 | 1.3187E-06 | 1.6523E-07 |
| | | R_u^1 | | 2.96999 | 2.99251 | 2.99892 | 2.99658 |
| | 0.1 | E_u | 4.9297E-04 | 6.2703E-05 | 7.8750E-06 | 9.8522E-07 | 1.2319E-07 |
| | | R_u^1 | | 2.97488 | 2.99319 | 2.99876 | 2.99953 |
| QFVE-1 | 0.2 | E_u | 5.2388E-04 | 6.6592E-05 | 8.3597E-06 | 1.0457E-06 | 1.3086E-07 |
| | | R_u^1 | | 2.97582 | 2.99383 | 2.99899 | 2.99842 |
| | 0.5 | E_u | 6.1107E-04 | 7.7931E-05 | 9.7902E-06 | 1.2247E-06 | 1.5342E-07 |
| | | R_u^1 | | 2.97108 | 2.99278 | 2.99895 | 2.99680 |
| | 0.9 | E_u | 6.5735E-04 | 8.3896E-05 | 1.0542E-05 | 1.3187E-06 | 1.6523E-07 |
| | | R_u^1 | | 2.96999 | 2.99251 | 2.99892 | 2.99658 |
| | 0.1 | E_u | 4.9668E-04 | 6.3296E-05 | 8.0014E-06 | 1.0243E-06 | 1.3406E-07 |
| | | R_u^1 | | 2.97211 | 2.98380 | 2.96568 | 2.93362 |
| | 0.2 | E_u | 5.2619E-04 | 6.6948E-05 | 8.4312E-06 | 1.0668E-06 | 1.3666E-07 |
| | | R_u^1 | | 2.97446 | 2.98923 | 2.98250 | 2.96460 |
| QFVE-2 | 0.5 | E_u | 6.1138E-04 | 7.7973E-05 | 9.7965E-06 | 1.2260E-06 | 1.5373E-07 |
| | | R_u^1 | | 2.97104 | 2.99262 | 2.99832 | 2.99551 |
| | 0.9 | E_u | 6.5736E-04 | 8.3897E-05 | 1.0542E-05 | 1.3187E-06 | 1.6523E-07 |
| | | R_u^1 | | 2.96999 | 2.99251 | 2.99892 | 2.99658 |
| | 0.1 | E_u | 4.8358E-04 | 6.6170E-05 | 1.0897E-05 | 2.2481E-06 | 4.3215E-07 |
| | | R_u^1 | | 2.86950 | 2.60230 | 2.27712 | 2.37910 |
| | 0.2 | E_u | 5.1682E-04 | 6.8178E-05 | 9.7474E-06 | 1.7606E-06 | 3.2209E-07 |
| | | R_u^1 | | 2.92227 | 2.80622 | 2.46895 | 2.45052 |
| | 0.5 | E_u | 6.0951E-04 | 7.7849E-05 | 9.8406E-06 | 1.2575E-06 | 1.6444E-07 |
| | | R_u^1 | | 2.96890 | 2.98385 | 2.96824 | 2.93488 |
| QFVE-3 | 0.9 | E_u | 6.5732E-04 | 8.3893E-05 | 1.0541E-05 | 1.3187E-06 | 1.6523E-07 |
| | | R_u^1 | | 2.96999 | 2.99250 | 2.99890 | 2.99654 |
| | 0.1 | E_u | 5.0009E-04 | 8.2417E-05 | 1.7586E-05 | 4.0042E-06 | 7.9228E-07 |
| | | R_u^1 | | 2.60119 | 2.22855 | 2.13480 | 2.33744 |
| | 0.2 | E_u | 5.2385E-04 | 7.5028E-05 | 1.3824E-05 | 2.9577E-06 | 5.7507E-07 |
| | | R_u^1 | | 2.80366 | 2.44027 | 2.22464 | 2.36264 |
| | 0.5 | E_u | 6.0883E-04 | 7.8074E-05 | 1.0018E-05 | 1.3420E-06 | 1.9249E-07 |
| | | R_u^1 | | 2.96311 | 2.96223 | 2.90012 | 2.80159 |
| | 0.9 | E_u | 6.5730E-04 | 8.3890E-05 | 1.0541E-05 | 1.3187E-06 | 1.6524E-07 |
| | | R_u^1 | | 2.96998 | 2.99249 | 2.99887 | 2.99647 |

where Mittag–Leffler function $E_{1,2-\alpha}(t)$ is defined by

$$E_{1,2-\alpha}(t) = \sum_{i=0}^{\infty} \frac{t^i}{\Gamma(i+2-\alpha)}.$$

In numerical calculation of this example, we use $\sum_{i=0}^{1000} t^i / \Gamma(i+2-\alpha)$ to approximate the Mittag–Leffler function $E_{1,2-\alpha}(t)$. The exact solution to the model is $u(\mathbf{x}, t) = e^t \sin(2\pi x) \sin(2\pi y)$. In Fig. 10, we draw contour plots for the absolute value of error between exact solution u and numerical solution u_h , i.e., $|u - u_h|$, with $\alpha = 0.5$, $h = 1/10$, $\Delta t = 1/2000$ at time $T = 1$ on Mesh I. It is obvious that accuracy of the first three schemes (QFE, QFVE-1, QFVE-2) is better than that of QFVE-3 and QFVE-4, see Tabs. 7, 8 for some detailed data.

3.4 Example 4

In the last example, we choose the nonlinear term $f(u) = u^3 - u$ and the source term $g(x, t) = 0$ with initial condition $u_0(\mathbf{x}) = x(1 - x^3)y(1 - y^3)$, where $\bar{\Omega} \times [0, T] = [0, 1]^2 \times [0, 1]$. Because of unknown exact solution, we take the numerical solution with $h = 1/160$, $\Delta t = 1/100$ as the ‘exact’ solution when computing the errors. The results are given in Tab. 9 where one can see that these schemes still work in this situation.

4 Conclusions

In this article, we study a nonlinear time-fractional Rayleigh-Stokes problem by using the quadratic finite volume element method combined with a specific time discretization. In temporal direction, we use a two step scheme to approximate the equation at time $t_{n-\alpha/2}$, where $L2-1_\sigma$ formula is used to approximate the time-fractional derivative. The fully discrete schemes of quadratic finite volume element are suggested and we find that only one of these schemes achieves the optimal convergence order in L^2 norm in space direction. We calculate some numerical examples by several kinds of quadratic finite volume element schemes and quadratic finite element scheme, space L^2 error orders of the QFE and QFVE-1 schemes reach 3. Meanwhile, numerical results of other three quadratic finite volume element schemes (QFVE-2, QFVE-3, QFVE-4) are nearly 2 and lower than the optimal order of QFVE-1. The future work includes the stability analysis and error estimates by following the related results on elliptic problems [46,48,54].

Acknowledgement: The authors would like to thank the editor and the anonymous reviewers for their valuable suggestions.

Funding Statement: This work was partially supported by the National Natural Science Foundation of China (No. 11871009).

Conflicts of Interest: The authors declare that they have no conflicts of interest to report regarding the present study.

References

1. Ma, J. T., Liu, J. Q., Zhou, Z. Q. (2014). Convergence analysis of moving finite element methods for space fractional differential equations. *Journal of Computational and Applied Mathematics*, 255(285), 661–670. DOI 10.1016/j.cam.2013.06.021.

2. Bu, W. P., Tang, Y. F., Yang, J. Y. (2014). Galerkin finite element method for two-dimensional Riesz space fractional diffusion equations. *Journal of Computational Physics*, 276, 26–38. DOI 10.1016/j.jcp.2014.07.023.
3. Wang, H., Du, N. (2013). A superfast-preconditioned iterative method for steady-state space-fractional diffusion equations. *Journal of Computational Physics*, 240(E), 49–57. DOI 10.1016/j.jcp.2012.07.045.
4. Liu, F., Zhuang, P., Turner, I., Burrage, K., Anh, V. (2014). A new fractional finite volume method for solving the fractional diffusion equation. *Applied Mathematical Modelling*, 38(15–16), 3871–3878. DOI 10.1016/j.apm.2013.10.007.
5. Feng, L. B., Zhuang, P., Liu, F., Turner, I. (2015). Stability and convergence of a new finite volume method for a two-sided space-fractional diffusion equation. *Applied Mathematics and Computation*, 257(1), 52–65. DOI 10.1016/j.amc.2014.12.060.
6. Pan, J. Y., Ng, M. K., Wang, H. (2016). Fast iterative solvers for linear systems arising from time-dependent space-fractional diffusion equations. *SIAM Journal on Scientific Computing*, 38(5), 2806–2826. DOI 10.1137/15M1030273.
7. Li, C., Zhao, S. (2016). Efficient numerical schemes for fractional water wave models. *Computers & Mathematics with Applications*, 71(1), 238–254. DOI 10.1016/j.camwa.2015.11.018.
8. Cheng, X. J., Duan, J. Q., Li, D. F. (2019). A novel compact ADI scheme for two-dimensional Riesz space fractional nonlinear reaction-diffusion equations. *Applied Mathematics and Computation*, 346(6), 452–464. DOI 10.1016/j.amc.2018.10.065.
9. Yin, B. L., Liu, Y., Li, H., He, S. (2019). Fast algorithm based on TT-M FE system for space fractional Allen-Cahn equations with smooth and non-smooth solutions. *Journal of Computational Physics*, 379(1), 351–372. DOI 10.1016/j.jcp.2018.12.004.
10. Yazdani, A., Mojahed, N., Babaei, A., Cendon, E. V. (2020). Using finite volume-element method for solving space fractional advection-dispersion equation. *Progress in Fractional Differentiation and Applications*, 6(1), 55–66. DOI 10.18576/pfda/060106.
11. Wang, Y. J., Liu, Y., Li, H., Wang, J. F. (2016). Finite element method combined with second-order time discrete scheme for nonlinear fractional Cable equation. *European Physical Journal Plus*, 131(61), 1–16. DOI 10.1140/epjp/i2016–16061–3.
12. Liu, Y., Yu, Z. D., Li, H., Liu, F. W., Wang, J. F. (2018). Time two-mesh algorithm combined with finite element method for time fractional water wave model. *International Journal of Heat and Mass Transfer*, 120(1), 1132–1145. DOI 10.1016/j.ijheatmasstransfer.2017.12.118.
13. Yin, B. L., Liu, Y., Li, H. (2020). A class of shifted high-order numerical methods for the fractional mobile/immobile transport equations. *Applied Mathematics and Computation*, 368(3), 124799. DOI 10.1016/j.amc.2019.124799.
14. Gao, G. H., Sun, H. W., Sun, Z. Z. (2015). Stability and convergence of finite difference schemes for a class of time-fractional sub-diffusion equations based on certain superconvergence. *Journal of Computational Physics*, 280, 510–528. DOI 10.1016/j.jcp.2014.09.033.
15. Alikhanov, A. A. (2015). A new difference scheme for the time fractional diffusion equation. *Journal of Computational Physics*, 280(1), 424–438. DOI 10.1016/j.jcp.2014.09.031.
16. Lin, Y. M., Li, X. J., Xu, C. J. (2011). Finite difference/spectral approximations for the fractional Cable equation. *Mathematics of Computation*, 80(275), 1369–1396. DOI 10.1090/S0025-5718-2010-02438-X.
17. Liu, F., Yang, C., Burrage, K. (2009). Numerical method and analytical technique of the modified anomalous subdiffusion equation with a nonlinear source term. *Journal of Computational and Applied Mathematics*, 231(1), 160–176. DOI 10.1016/j.cam.2009.02.013.
18. Cao, X. N., Cao, X. X., Wen, L. P. (2016). The implicit midpoint method for the modified anomalous sub-diffusion equation with a nonlinear source term. *Journal of Computational and Applied Mathematics*, 318, 199–210. DOI 10.1016/j.cam.2016.10.014.
19. Tuan, N. H., Zhou, Y., Thach, T. N., Can, N. H. (2019). Initial inverse problem for the nonlinear fractional Rayleigh-Stokes equation with random discrete data. *Communications in Nonlinear Science and Numerical Simulation*, 78(5), 104873. DOI 10.1016/j.cnsns.2019.104873.

20. Zhou, Y., Wang, J. N. (2019). The nonlinear Rayleigh-Stokes problem with Riemann–Liouville fractional derivative. *Mathematical Methods in the Applied Sciences*, 1–8(3), 2431–2438. DOI 10.1002/mma.5926.
21. Guan, Z., Wang, X. D., Ouyang, J. (2020). An improved finite difference/finite element method for the fractional Rayleigh-Stokes problem with a nonlinear source term. *Journal of Applied Mathematics and Computing*, 65, 1–29. DOI 10.1007/s12190-020-01399-4.
22. Bao, N. T., Hoang, L. N., van, A. V., Nguyen, H. T., Zhou, Y. (2020). Existence and regularity of inverse problem for the nonlinear fractional Rayleigh-Stokes equations. *Mathematical Methods in the Applied Sciences*, 44(1), 1–27. DOI 10.1002/mma.6162.
23. Sayevand, K., Arjang, F. (2016). Finite volume element method and its stability analysis for analyzing the behavior of sub-diffusion problems. *Applied Mathematics and Computation*, 290(2), 224–239. DOI 10.1016/j.amc.2016.06.008.
24. Karaa, S., Mustapha, K., Pani, A. K. (2016). Finite volume element method for two-dimensional fractional subdiffusion problems. *IMA Journal of Numerical Analysis*, 37, 945–964. DOI 10.1093/imanum/drw010.
25. Karaa, S., Pani, A. K. (2018). Error analysis of a finite volume element method for fractional order evolution equations with nonsmooth initial data. *ESAIM Mathematical Modelling and Numerical Analysis*, 52(2), 773–801. DOI 10.1051/m2an/2018029.
26. Badr, M., Yazdani, A., Jafari, H. (2018). Stability of a finite volume element method for the time-fractional advection-diffusion equation. *Numerical Methods for Partial Differential Equations*, 34(5), 1459–1471. DOI 10.1002/num.22243.
27. Zhao, J., Li, H., Fang, Z. C., Liu, Y. (2019). A mixed finite volume element method for time-fractional reaction-diffusion equations on triangular grids. *Mathematics*, 7(7), 600. DOI 10.3390/math7070600.
28. Zhao, J., Fang, Z. C., Li, H., Liu, Y. (2020). Finite volume element method with the WSGD formula for nonlinear fractional mobile/immobile transport equations. *Advances in Difference Equations*, 360, 1–20. DOI 10.1186/s13662-020-02786-8.
29. Zhang, Y. L., Yin, B. L., Cao, Y., Liu, Y., Li, H. (2020). A numerical algorithm based on quadratic finite element for two-dimensional nonlinear time fractional thermal diffusion model. *Computer Modeling in Engineering & Sciences*, 122(3), 1081–1098. DOI 10.32604/cmes.2020.07822.
30. Wu, G. C. (2011). A fractional characteristic method for solving fractional partial differential equations. *Applied Mathematics Letters*, 24(7), 1046–1050. DOI 10.1016/j.aml.2011.01.020.
31. Li, C. P., Zhao, Z. G., Chen, Y. Q. (2011). Numerical approximation of nonlinear fractional differential equations with subdiffusion and superdiffusion. *Computers & Mathematics with Applications*, 62(3), 855–875. DOI 10.1016/j.camwa.2011.02.045.
32. Feng, L. B., Zhuang, P., Liu, F., Turner, I., Gu, Y. T. (2015). Finite element method for space-time fractional diffusion equation. *Numerical Algorithms*, 72(3), 749–767. DOI 10.1007/s11075-015-0065-8.
33. Fan, W. P., Liu, F. W., Jiang, X. Y., Turner, I. (2017). A novel unstructured mesh finite element method for solving the time-space fractional wave equation on a two-dimensional irregular convex domain. *Fractional Calculus and Applied Analysis*, 20(2), 352–383. DOI 10.1515/fca-2017-0019.
34. Zhang, H., Jiang, X. Y., Yang, X. (2018). A time-space spectral method for the time-space fractional Fokker–Planck equation and its inverse problem. *Applied Mathematics and Computation*, 320(1), 302–318. DOI 10.1016/j.amc.2017.09.040.
35. Fetecau, C., Zierep, J. (2001). On a class of exact solutions of the equations of motion of a second grade fluid. *Acta Mechanica*, 150(1–2), 135–138. DOI 10.1007/BF01178551.
36. Tan, W. C., Masuoka, T. (2005). Stokes’ first problem for a second grade fluid in a porous half-space with heated boundary. *International Journal of Non-Linear Mechanics*, 40(4), 515–522. DOI 10.1016/j.ijnonlinmec.2004.07.016.
37. Shen, F., Tan, W. C., Zhao, Y. H., Masuoka, T. (2006). The Rayleigh-Stokes problem for a heated generalized second grade fluid with fractional derivative model. *Nonlinear Analysis: Real World Applications*, 7(5), 1072–1080. DOI 10.1016/j.nonrwa.2005.09.007.
38. Zierep, J., Fetecau, C. (2007). Energetic balance for the Rayleigh-Stokes problem of a Maxwell fluid. *International Journal of Engineering Science*, 45(2), 617–627. DOI 10.1016/j.ijengsci.2007.04.015.

39. Parvizi, M., Khodadadian, A., Eslahchi, M. (2020). Analysis of Ciarlet-Raviart mixed finite element methods for solving damped Boussinesq equation. *Journal of Computational and Applied Mathematics*, 379(1), 112818. DOI 10.1016/j.cam.2020.112818.
40. Abbaszadeh, M., Dehghan, M., Khodadadian, A., Heitzinger, C. (2019). Analysis and application of the interpolating element free Galerkin (IEFG) method to simulate the prevention of groundwater contamination with application in fluid flow. *Journal of Computational and Applied Mathematics*, 368(155), 112453. DOI 10.1016/j.cam.2019.112453.
41. Abbaszadeh, M., Dehghan, M., Khodadadian, A., Noii, N., Heitzinger, C. et al. (2020). A reduced-order variational multiscale interpolating element free Galerkin technique based on proper orthogonal decomposition for solving Navier–Stokes equations coupled with a heat transfer equation: Nonstationary incompressible Boussinesq equations. *Journal of Computational Physics*, 426(2), 109875. DOI 10.1016/j.jcp.2020.109875.
42. Tian, M. Z., Chen, Z. Y. (1991). Quadratic element generalized differential methods for elliptic equations. *Numerical Mathematics a Journal of Chinese Universities*, 13, 99–113. DOI CNKI: SUN: GDSX. 0.1991-02-000.
43. Liebau, F. (1996). The finite volume element method with quadratic basis functions. *Computing*, 57(4), 281–299. DOI 10.1007/BF02252250.
44. Xu, J. C., Zou, Q. S. (2009). Analysis of linear and quadratic simplicial finite volume methods for elliptic equations. *Numerische Mathematik*, 111(3), 469–492. DOI 10.1007/s00211-008-0189-z.
45. Chen, Z. Y., Wu, J. F., Xu, Y. S. (2012). Higher-order finite volume methods for elliptic boundary value problems. *Advances in Computational Mathematics*, 37(2), 191–253. DOI 10.1007/s10444-011-9201-8.
46. Wang, X., Li, Y. H. (2016). L^2 error estimates for high order finite volume methods on triangular meshes. *SIAM Journal on Numerical Analysis*, 54(5), 2729–2749. DOI 10.1137/140988486.
47. Zou, Q. S. (2017). An unconditionally stable quadratic finite volume scheme over triangular meshes for elliptic equations. *Journal of Scientific Computing*, 70(1), 112–124. DOI 10.1007/s10915-016-0244-3.
48. Zhou, Y. H., Wu, J. M. (2020). A family of quadratic finite volume element schemes over triangular meshes for elliptic equations. *Computers & Mathematics with Applications*, 79(9), 2473–2491. DOI 10.1016/j.camwa.2019.11.017.
49. Zhou, Y. H., Wu, J. M. (2020). A unified analysis of a class of quadratic finite volume element schemes on triangular meshes. *Advances in Computational Mathematics*, 46(5), 777. DOI 10.1007/s10444-020-09809-8.
50. Wang, P., Zhang, Z. Y. (2010). Quadratic finite volume element method for the air pollution model. *International Journal of Computer Mathematics*, 87(13), 2925–2944. DOI 10.1080/00207160802680663.
51. Jin, G. H., Li, H. G., Zhang, Q. H., Zou, Q. S. (2016). Linear and quadratic finite volume methods on triangular meshes for elliptic equations with singular solutions. *International Journal of Numerical Analysis and Modeling*, 13(2), 244–264.
52. Xiong, Z. G., Deng, K. (2017). A quadratic triangular finite volume element method for a semilinear elliptic equation. *Advances in Applied Mathematics and Mechanics*, 9(1), 186–204. DOI 10.4208/aamm.2014.m63.
53. Du, Y. W., Li, Y. H., Sheng, Z. Q. (2019). Quadratic finite volume method for a nonlinear elliptic problem. *Advances in Applied Mathematics and Mechanics*, 11(4), 838–869. DOI 10.4208/aamm.OA-2017-0231.
54. Zhou, Y. H. (2020). A class of bubble enriched quadratic finite volume element schemes on triangular meshes. *International Journal of Numerical Analysis and Modeling*, 17(6), 872–899.